



저작자표시-비영리-변경금지 2.0 대한민국

이용자는 아래의 조건을 따르는 경우에 한하여 자유롭게

- 이 저작물을 복제, 배포, 전송, 전시, 공연 및 방송할 수 있습니다.

다음과 같은 조건을 따라야 합니다:



저작자표시. 귀하는 원저작자를 표시하여야 합니다.



비영리. 귀하는 이 저작물을 영리 목적으로 이용할 수 없습니다.



변경금지. 귀하는 이 저작물을 개작, 변형 또는 가공할 수 없습니다.

- 귀하는, 이 저작물의 재이용이나 배포의 경우, 이 저작물에 적용된 이용허락조건을 명확하게 나타내어야 합니다.
- 저작권자로부터 별도의 허가를 받으면 이러한 조건들은 적용되지 않습니다.

저작권법에 따른 이용자의 권리는 위의 내용에 의하여 영향을 받지 않습니다.

이것은 [이용허락규약\(Legal Code\)](#)을 이해하기 쉽게 요약한 것입니다.

[Disclaimer](#)

공학석사 학위논문

**Solid-Moderated Core Design  
Using Low-Enriched Uranium  
Modeling Fuel for Kyoto University  
Critical Assembly**

저농축 모의 핵연료를 이용한  
교토대 고체 감속 임계집합체 노심 설계

2020년 8월

서울대학교 대학원  
에너지시스템공학부  
송 교 성

**Solid-Moderated Core Design  
Using Low-Enriched Uranium  
Modeling Fuel for Kyoto University  
Critical Assembly**

저농축 모의 핵연료를 이용한  
교토대 고체 감속 임계집합체 노심 설계

지도 교수 심형진

이 논문을 공학석사 학위논문으로 제출함  
2020년 8월

서울대학교 대학원  
에너지시스템공학부  
송교성

송교성의 공학석사 학위논문을 인준함  
2020년 8월

위원장                     주한규                    (인)

부위원장                     심형진                    (인)

위원                     변철호                    (인)

# Abstract

For the Kyoto University Critical Assembly (KUCA), feasibility studies on its conversion from highly-enriched uranium (HEU) fuel to low-enriched uranium (LEU) one have been numerically conducted, recently. The main objective of this research is to design two cores using the LEU modeling fuels, which are composed of the current HEU and natural uranium (NU) fuels – the thermal spectrum core and fast-thermal hybrid spectrum core, as a feasibility study for the LEU conversion for the solid-moderated core of KUCA. And, the number of HEU plates used in the designed cores is set to less than 5,000 plates. In this research, the cores with the LEU modeling fuel are designed by a Monte Carlo (MC) neutron transport analysis code, McCARD. McCARD calculations are conducted to analyze criticality and neutron spectra of the cores. And, they are evaluated whether the designed cores can meet the safety regulations for implementation at the KUCA.

The thermal spectrum core with the LEU modeling fuel is designed. The ratio of  $^1\text{H}$  to  $^{235}\text{U}$  in the LEU modeling unit cell is set to 200 or higher to make a thermal spectrum. The LEU modeling cell used in the LEU modeling fuel assembly consists of four HEU plates, one NU plate and nine PE plates. The thermal spectrum core is composed of 31 LEU modeling fuel assemblies. The total number of HEU plates used in the core is 1,720 plates. Compared to the spectrum of a typical polyethylene-moderated configuration of the EE1 core at KUCA, a softened spectrum can be achieved in the thermal spectrum core. McCARD calculations are conducted to estimate the excess reactivity ( $\rho_{ex}$ ), control rod worth, secondary shutdown reactivity ( $\rho_{SD2}$ ), differential reactivity, which is an inserted reactivity per second when a control rod is withdrawn from the critical position, and the isothermal temperature coefficient (ITC). The thermal spectrum core satisfies all the regulatory requirements but the positive ITC is closed to the regulatory requirement of ITC. To reduce ITC, the reflector element used in the core is changed from polyethylene (PE) to graphite (Gr). By varying the reflector element from PE to Gr, the ITC decreases 19.6 pcm/K to 13.5 pcm/K. Also, the thermal spectrum core with the Gr reflector satisfies all the regulatory requirements. From the design analyses, the thermal spectrum core is found feasible with the use of the LEU modeling fuel at KUCA.

The LEU modeling fuel assembly used in the fast-thermal hybrid spectrum core is designed without the moderator to make a fast spectrum. The core with the only LEU modeling fuel assemblies is hard to reach criticality. Therefore, the designed fast-thermal hybrid spectrum core has two different regions – a driver region and a test region. The test region is composed of the LEU modeling fuel assemblies. And, the driver region consists of the typical HEU fuel assemblies in the KUCA core, which is composed of HEU plates and polyethylene plates, to have the core achieve criticality. The total number of HEU plates used in the core is 4,608 plates. Compared to the spectrum of the thermal spectrum core, a hardened spectrum is achieved in the test region of the hybrid spectrum core. The fast-thermal hybrid spectrum core satisfies all the regulatory requirements except ITC considering its 95% confidence intervals. To reduce ITC, the Gr-reflected fast-thermal hybrid spectrum core is designed. By varying the reflector element from PE to Gr, the ITC decreases from 19.8 pcm/K to 3.6 pcm/K. Also, the fast-thermal hybrid spectrum core with Gr reflectors satisfies all the regulatory requirements. From the design analyses, the LEU modeling fuel assembly without the moderator present difficulty in achieving criticality in the fast spectrum core but the fast-thermal hybrid spectrum core is found feasible with the use of the LEU modeling fuel at KUCA.

To analyze the sensitivity for ITC of the system temperature, the MC  $k$ -eigenvalue calculations are conducted for the hybrid spectrum core at different system temperatures. The estimated ITCs exceed 20 pcm/K, which is a regulatory requirement of solid-moderated core in KUCA, due to the effect of the spectral shift of thermal neutrons. To reduce ITC, four cores with the regional Gr reflector rods are analyzed. With these results, it can be concluded that the reflector element surrounding the core can be suggested to change from PE to Gr reflector to reduce ITC.

**Keyword:** LEU Modeling Fuel, Natural Uranium, Solid-Moderated Core, Neutron Spectrum, Isothermal Temperature Coefficient, KUCA, McCARD

**Student Number:** 2018-28054

# Contents

<b>Abstract .....</b>	<b>i</b>
<b>Contents.....</b>	<b>iii</b>
<b>List of Figures .....</b>	<b>iv</b>
<b>List of Tables .....</b>	<b>vi</b>
<b>Chapter 1. Introduction .....</b>	<b>1</b>
1.1. Background and Purpose.....	1
1.2. Organization of Thesis .....	2
<b>Chapter 2. Thermal Spectrum Core .....</b>	<b>3</b>
2.1 Low-Enriched Uranium Modeling Fuel.....	3
2.2 Polyethylene-Moderated Core.....	5
2.3 Graphite-Reflected Core .....	1 3
<b>Chapter 3. Fast-Thermal Hybrid Spectrum Core Design .....</b>	<b>2 1</b>
3.1 Low-Enriched Uranium Modeling Fuel.....	2 1
3.2 Polyethylene-Moderated Core.....	2 4
3.3 Graphite-Reflected Core .....	3 1
<b>Chapter 4. Isothermal Temperature Coefficient.....</b>	<b>4 0</b>
4.1 Sensitivity for ITC of System Temperature .....	4 0
4.2 Sensitivity for ITC of Regional Reflector Element.....	4 1
<b>Chapter 5. Conclusion .....</b>	<b>4 6</b>
<b>References.....</b>	<b>4 8</b>
<b>초 록 .....</b>	<b>5 3</b>

# List of Figures

Fig. 2-1 Layout of the LEU modeling unit cell .....	3
Fig. 2-2 The LEU modeling fuel assembly, S14 .....	5
Fig. 2-3 The active core region of S14.....	5
Fig. 2-4 The thermal spectrum core configuration.....	6
Fig. 2-5 Tally positions for neutron energy spectrum analyses .....	7
Fig. 2-6 The D60 assembly used in the EE1 core .....	7
Fig. 2-7 Neutron spectra for (a) the thermal spectrum core and (b) the EE1 core ..	8
Fig. 2-8 Integral rod worth curves for the thermal spectrum core.....	1 0
Fig. 2-9 Neutron spectra for the reflector and moderator regions of the thermal spectrum core at 300 K and 350 K.....	1 2
Fig. 2-10 Microscopic capture cross section of hydrogen.....	1 3
Fig. 2-11 The S14 assembly used in the Gr-reflected thermal spectrum core.....	1 4
Fig. 2-12 The Gr-reflected thermal spectrum core configuration .....	1 4
Fig. 2-13 Tally positions for neutron energy spectrum analyses .....	1 5
Fig. 2-14 Neutron spectra for (a) the Gr-reflected core and (b) the PE-reflected core .....	1 5
Fig. 2-15 Integral rod worth curves for the Gr-reflected thermal spectrum core	1 7
Fig. 2-16 Neutron spectra for the reflector and moderator regions of the Gr-reflected thermal spectrum core at 300 K and 350 K.....	1 9
Fig. 2-17 Microscopic capture cross section of hydrogen and carbon .....	2 0
Fig. 3-1 $k_{inf}$ sensitivities of the number of LEU modeling unit cells stacked in the test assembly .....	2 1
Fig. 3-2 The preliminary hybrid spectrum core configuration .....	2 2
Fig. 3-3 $k$ sensitivities of the number of LEU modeling unit cells stacked in the LEU modeling fuel assembly.....	2 3
Fig. 3-4 The T24 assembly used in the fast-thermal hybrid spectrum core .....	2 4
Fig. 3-5 The active core region in T24.....	2 4
Fig. 3-6 Hybrid spectrum core configuration.....	2 5
Fig. 3-7 Tally positions for neutron energy spectrum analyses .....	2 6

Fig. 3-8 Neutron spectra for (a) upper driver region, (b) test region, (c) lower driver region and (d) the thermal spectrum core.....	2 6
Fig. 3-9 Integral rod worth curves of the hybrid spectrum core.....	2 8
Fig. 3-10 Neutron spectra for the reflector and moderator regions of the hybrid spectrum core at 300 K and 350 K.....	3 0
Fig. 3-11 The Gr-reflected hybrid spectrum core configuration .....	3 2
Fig. 3-12 The D60 assembly used in the Gr-reflected hybrid spectrum core.....	3 3
Fig. 3-13 The T24 assembly used in the Gr-reflected hybrid spectrum core .....	3 3
Fig. 3-14 Tally positions for neutron energy spectrum analyses.....	3 3
Fig. 3-15 Neutron spectra for (a) upper driver region [D60; Gr], (b) test region [T24; Gr], (c) lower driver region [D20; Gr] and (d) test region [T24; PE] .....	3 4
Fig. 3-16 Integral rod worth curve for the Gr-reflected hybrid spectrum core ...	3 6
Fig. 3-17 Neutron spectra for the reflector and moderator regions of the Gr-reflected hybrid spectrum core at 300 K and 350 K.....	3 8
Fig. 4-1 Temperature-dependent $k_{\text{eff}}$ for the hybrid spectrum core .....	4 0
Fig. 4-2 Temperature-dependent ITC of the hybrid spectrum core.....	4 1
Fig. 4-4 Core configurations of the hybrid spectrum core with the Gr reflectors	4
2	
Fig. 4-5 Core configurations of thermal spectrum core with the Gr reflectors ...	4 4
Fig. B-1 The D04 assembly used in hybrid spectrum core .....	5 1
Fig. B-2 The D20 assembly used in Gr-reflected hybrid spectrum core.....	5 1
Fig. B-3 the S10 assembly used in thermal spectrum core .....	5 1
Fig. B-4 The S07 assembly used in Gr-reflected thermal spectrum core.....	5 1
Fig. B-5 The Gr reflector rod .....	5 2
Fig. B-6 The outer PE reflector rod.....	5 2
Fig. B-7 The inner PE reflector rod.....	5 2

# List of Tables

Table 2-1 Atomic densities of fuel plates .....	4
Table 2-2 Specifications of the LEU modeling unit cell .....	4
Table 2-3 Specifications of the active core according to the number of the PE plates .....	4
Table 2-4 Regulatory requirements of KUCA A-core and McCARD calculation results of the thermal spectrum core.....	9
Table 2-5 Region-wise and isotope-wise contributions of each isotope to ITC of the thermal spectrum core .....	1 1
Table 2-6 Regulatory requirements of KUCA A-core and McCARD calculation results of the Gr-reflected thermal spectrum core .....	1 6
Table 2-7 Region-wise contribution of thermal scattering cross section to ITC of the thermal spectrum core .....	1 8
Table 3-1 Regulatory requirements of KUCA A-core and McCARD calculation results of the hybrid spectrum core .....	2 7
Table 3-2 Region-wise and isotope-wise contribution of each isotope to ITC of the hybrid spectrum core.....	2 9
Table 3-3 Regulatory requirements of KUCA A-core and McCARD calculation results of the Gr-reflected hybrid spectrum core.....	3 5
Table 3-4 Region-wise and isotope-wise of each isotope to ITC of the Gr-reflected hybrid spectrum core.....	3 7
Table 4-1 Effective multiplication factor of the Gr-reflected hybrid spectrum cores .....	4 3
Table 4-2 ITC of the Gr-reflected hybrid spectrum cores .....	4 3
Table 4-3 Effective multiplication factor of the Gr-reflected thermal spectrum cores .....	4 5
Table 4-4 ITC of Gr-reflected thermal spectrum cores .....	4 5
Table A-1. Atomic densities of polyethylene (PE) plates.....	5 0
Table A-2. Atomic densities of polyethylene (p) plates .....	5 0
Table A-3. Atomic densities of graphite (Gr).....	5 0

# Chapter 1. Introduction

## 1.1. Background and Purpose

The Reduced Enrichment for Research and Test Reactor (RERTR) Program has been driving to develop the technologies necessary to enable the conversion of research reactors using highly-enriched uranium (HEU) to low-enriched uranium (LEU) fuels since 1978 [1-3]. During the program, dozens of research reactors have been converted from HEU to LEU fuels. The SAFARI-1 [4] reactor which is a 20 MW tank-in pool type light water reactor was fully converted to LEU fuels in 2009. The conversion to LEU of the GHARR-1 [5] reactor was completed in 2016. For the Kyoto University Critical Assembly (KUCA), feasibility studies [6-7] in its conversion from HEU to LEU one have been numerically, recently.

KUCA has been operated for research and education since 1974. KUCA has two solid-moderated and –reflected cores (A- and B-cores) and one light water-moderated and –reflected core (C-core). The solid-moderated cores use highly-enriched Uranium (HEU; 93 wt%) fuels and polyethylene (PE) plates as the moderator and reflector. A wide range of neutron spectra could be achieved by varying the combination of fuel and moderator plates in fuel assemblies, and reflector materials. For the light water-moderated core, fuel assemblies are placed in a water tank and the reflector region could be substituted with a heavy-water reflector. The neutron spectra of the water-moderated core could be controlled by varying the fuel loading pitch.

The objective of this research is to design two cores using the LEU modeling fuels, which are composed of the current HEU and natural uranium (NU) fuels – the thermal spectrum core and fast-thermal hybrid spectrum core (Hybrid spectrum core hereafter), as a feasibility study for the LEU conversion at the KUCA. The newly designed cores are implemented for the KUCA A-core, the solid-moderated and –reflected core. The number of HEU plates used in the cores is set to less than 5,000 plates. The cores are designed by a Monte Carlo (MC) neutron transport analysis code, McCARD [8]. McCARD calculations are conducted to analyze criticality and neutron spectra. Also, they are evaluated whether the designed cores can meet the

safety regulations for implementation at the KUCA:

- Excess reactivity ( $\rho_{ex}$ )  $\leq$  350 pcm
- $\rho_{ex} + 1000$  pcm  $\leq$   $\sum_i^3 (C_i \text{ rod worth})$
- (Rod worth) $_{\max} \leq \frac{1}{3}$ (All control and safety rod worth)
- Differential reactivity  $\leq$  20 pcm/s
- Shutdown reactivity ( $\rho_{SD2}$ )  $\geq$  125 % of  $\rho_{ex}$
- Isothermal temperature coefficient (ITC)  $\leq$  20 pcm/K

The differential reactivity is an inserted reactivity per second when a control rod is withdrawn from critical position. The secondary shutdown reactivity is the shutdown reactivity by a secondary shutdown system which is dropping three fuel assemblies and six reflector rods. In addition, the sensitivities of ITC will be analyzed by varying the system temperature and reflector elements from PE to Gr in order to reduce ITC.

## 1.2. Organization of Thesis

In Chapter 2.1, the LEU modeling fuel used in the thermal spectrum core is presented. In Chapter 2.2, the designed thermal spectrum core with the LEU modeling fuel assembly is introduced and its neutronics parameters are presented. By varying the reflector element from PE to Gr, the graphite-reflected thermal spectrum core is described in Chapter 2.3. The LEU modeling fuel used in the fast-thermal hybrid spectrum core is presented in Chapter 3.1. From Chapter 3.2 to Chapter 3.3, the PE-reflected and Gr-reflected hybrid spectrum cores are described, respectively. Chapter 4 provides the sensitivities of the ITC to the system temperature and the regional reflector elements to reduce the ITC.

## Chapter 2. Thermal Spectrum Core

### 2.1 Low-Enriched Uranium Modeling Fuel

A fuel assembly stacking solid plates inside an aluminum sheath (55.3×55.3×1524 mm) is composed of fuel region, lower and upper polyethylene reflectors. A wide variety of neutron spectra could be achieved according to the combination of fuel and moderator plates used in a unit cell. The unit cells are stacked in the active core.

The LEU modeling unit cell stacked in the fuel assembly is composed of four HEU plates and one NU plate (1/16"HEU×2+1.05 mm thick NU+1/16"HEU×2) to have an enrichment of 17.0 wt% as the unit cell average value. Since the density of the NU plate is about 30 times greater than that of the HEU plates, the average enrichment of the LEU modeling unit cell is less than 20 wt%. Figure 2-1 shows the layout of the LEU modeling unit cell. The total thickness of the unit cell is 7.4 mm. Details of the material of HEU and NU plates are shown in Table 2-1 and Table 2-2.

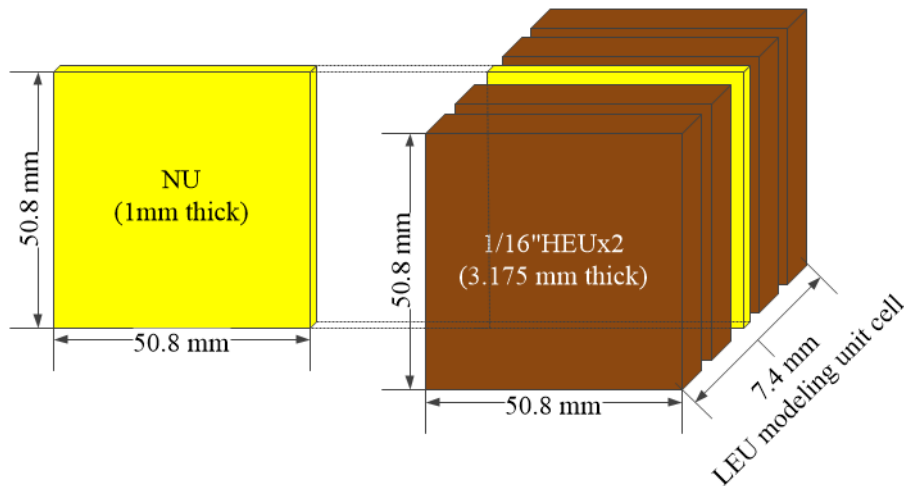


Fig. 2-1 Layout of the LEU modeling unit cell (1/16"HEU×2+1.05 mm thick NU+1/16"HEU×2)

Table 2-1 Atomic densities of fuel plates

Fuel	Isotope	Atomic density [ $\times 10^{24}/\text{cm}^3$ ]
1/16"HEU×2 (3.175 mm thick)	$^{234}\text{U}$	1.13659E-05
	$^{235}\text{U}$	1.50682E-03
	$^{236}\text{U}$	4.82971E-06
	$^{238}\text{U}$	9.25879E-05
	$^{27}\text{Al}$	5.56436E-02
NU (1.05 mm thick)	$^{235}\text{U}$	3.25792E-04
	$^{238}\text{U}$	4.48577E-02

Table 2-2 Specifications of the LEU modeling unit cell

Fuel Plates	1/16"HEU×4	1 mm thick NU	The LEU modeling unit cell
Enrichment	93.20 wt%	0.71 wt%	17.00 wt%
Thickness	0.635 cm	0.105 cm	0.740 cm
Volume	16.387 $\text{cm}^3$	2.170 $\text{cm}^3$	19.097 $\text{cm}^3$
Density	0.63 $\text{g}/\text{cm}^3$	17.86 $\text{g}/\text{cm}^3$	3.08 $\text{g}/\text{cm}^3$

To make a core with a thermal spectrum, the LEU modeling cell is designed to use the PE plates as the moderator with the previous LEU modeling cell. The ratio of  $^1\text{H}$  to  $^{235}\text{U}$  in the LEU modeling unit cell is set to 200 or higher. And, the length of the active core comprising of the LEU modeling unit cells is set to 500 mm. The ratio according to the number of 1/8" PE (3.158 mm thick) plates is shown in Table 2-3.

Table 2-3 Specifications of the active core according to the number of the PE plates

The LEU modeling unit cell	Candidates			
The number of 1/8" PE plates	8	9	10	11
$^1\text{H}/^{235}\text{U}$	198.3	223.1	247.9	272.7
The thickness of unit cell [mm]	32.664	35.822	38.980	42.138
The number of unit cells stacked in the active core	15	14	13	12
The length of the active core [mm]	489.960	501.508	506.740	505.656

The number of 1/8" PE plates used in the LEU modeling unit cell and that of the LEU modeling unit cells stacked in the fuel assembly are determined to 9 and 14, respectively, because they satisfy the set point of the ratio and make the length of the active core is close to 500 mm. In other words, the active core of the LEU modeling fuel assembly is composed of 14 LEU modeling unit cells ((1/16"HEU×2+1.05 mm thick NU+1/16"HEU×2) + 1/8"PE×9). The LEU modeling fuel assembly with a softened spectrum (S14) and its active core region are shown in Figs. 2-2 and 2-3, respectively. The lower and upper reflectors in S14 are composed of PE plates. To assess the infinite multiplication factor ( $k_{inf}$ ) of S14, the McCARD  $k$ -eigenvalue calculation is performed on 500 inactive and 1,000 active cycles with 100,000 histories per cycle using ENDF/B-VIII.0 [9] cross section libraries. The infinite multiplication factor of the single S14 assembly with reflective boundary conditions is  $1.45941 \pm 0.00005$ .

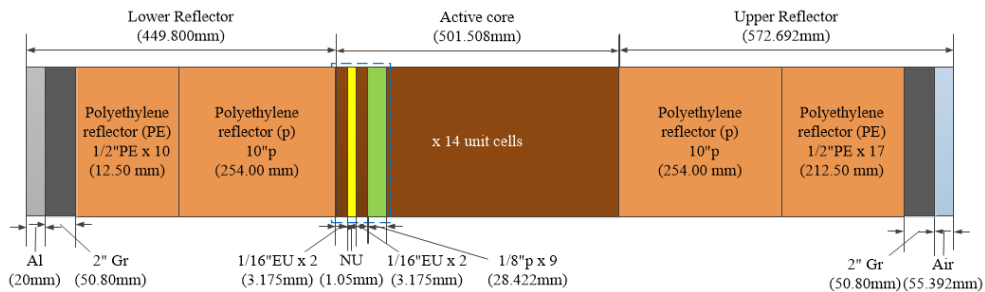


Fig. 2-2 The LEU modeling fuel assembly, S14

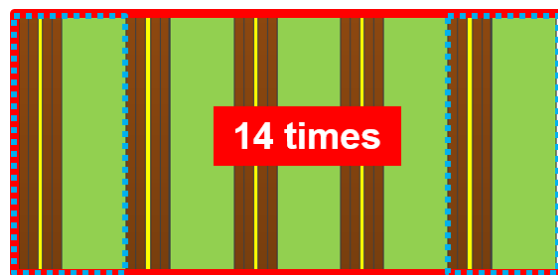


Fig. 2-3 The active core region of S14

## 2.2 Polyethylene-Moderated Core

### 2.2.1 Core Description

As shown in Fig. 2-4, the designed thermal spectrum core is composed of 30

S14 assemblies and one S10 assembly which is composed of 10 times LEU modeling unit cells. Note that 10 unit cells in S10 are determined to have the core reach its critical mass. The total number of HEU plates used in the core is 1,720 plates. The fuel assemblies are surrounded by the PE reflector elements. There are 3 control rods (C1, C2 and C3) and 3 safety rods (S4, S5 and S6). The SD2 region is a secondary shutdown system which is dropping the SD2 region.

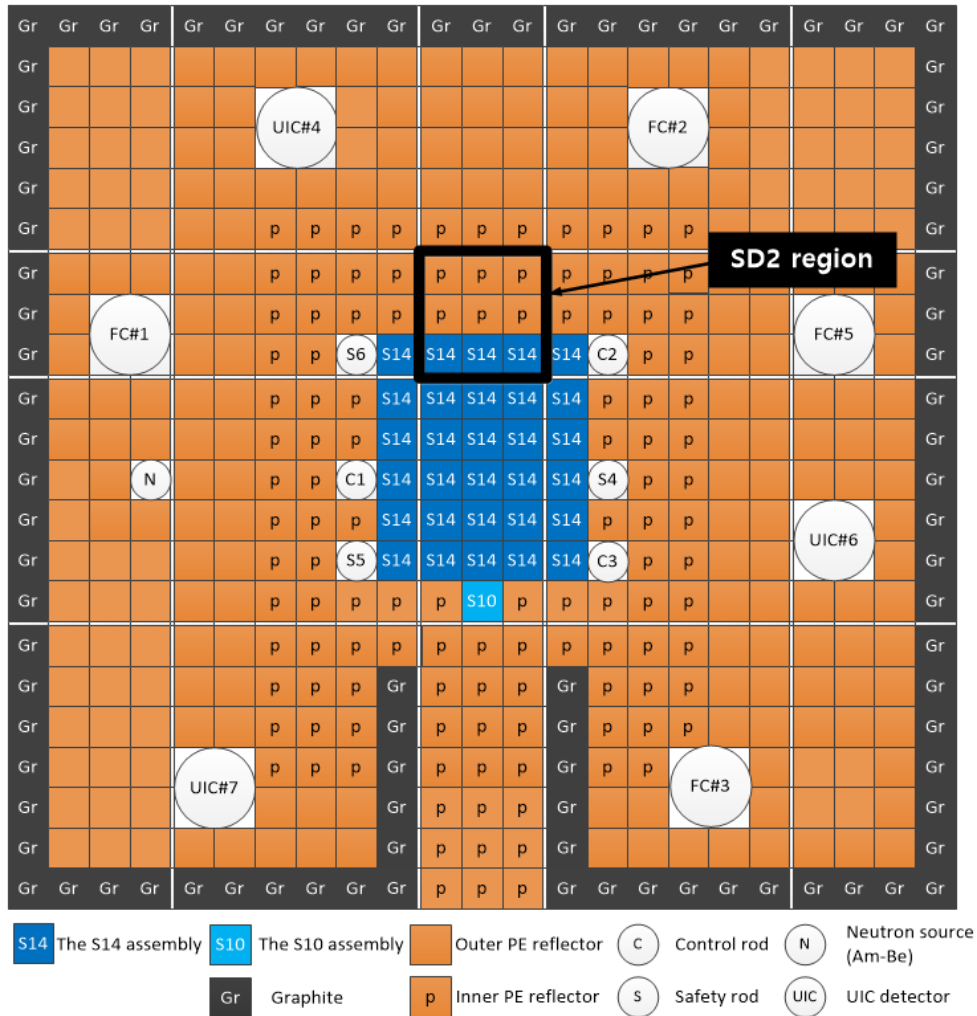


Fig. 2-4 The thermal spectrum core configuration

## 2.2.2 Neutron Spectrum

To verify a thermal spectrum of the designed core, one representative position to check their neutron energy spectrum is chosen as shown on the left side of Fig. 2-

5 (a). In addition, the spectrum of the core is compared with that of a typical PE-moderated core configuration of the EE1 core [10] comprising 25 D60 assemblies as shown on the right side of Fig. 2-5 (b). In the D60 assembly, the fuel unit cells composed of two 3.175 mm (1/8”) thick HEU plates and a 3.158 mm (1/8”) thick PE plate are stacked as many as 60. The length of the active core is about 38 cm and the lower and upper reflectors in D60 are composed of PE plates as shown in Fig. 2-6.

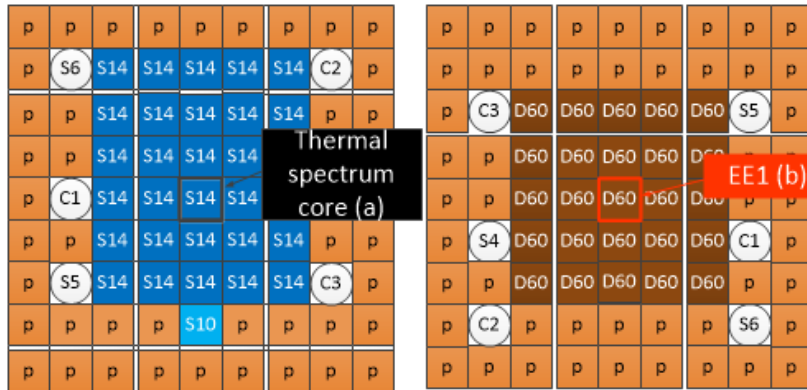


Fig. 2-5 Tally positions for neutron energy spectrum analyses (Left: the thermal spectrum core, Right: the EE1 core)

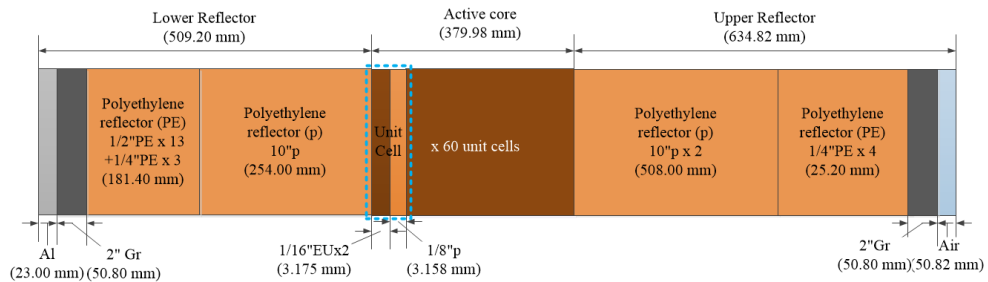


Fig. 2-6 The D60 assembly used in the EE1 core

In the MC eigenvalue calculations, neutron spectra are tallied for two unit cells located in the middle height of each fuel assembly position. The neutron energy spectrum is normalized to

$$\int_0^{\infty} \phi(E) dE = 1. \quad (2.1)$$

Figure 2-7 shows comparisons of each regional spectrum. From the figure, one can see that a thermal spectrum can be achieved in the thermal spectrum core (a)

because the PE plates are used as many as 9 in the fuel unit cells of S14 as a moderator.

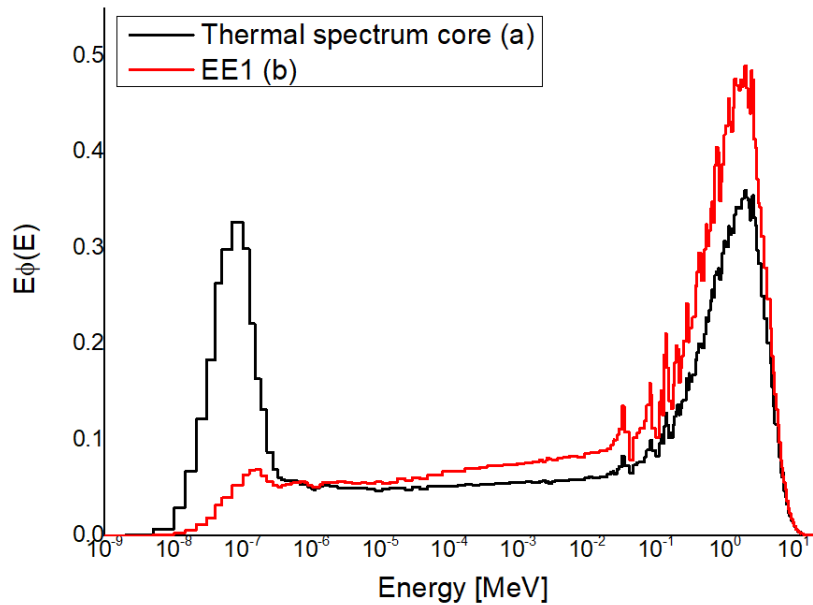


Fig. 2-7 Neutron spectra for (a) the thermal spectrum core and (b) the EE1 core

### 2.2.3 Neutronics Parameters

The second column of Table 2-4 shows regulatory requirements that should be met to operate the KUCA A-core. In the table, differential reactivity is an inserted reactivity per second when a control rod is withdrawn or inserted from critical position.  $\rho_{SD2}$  is the shutdown reactivity by a secondary shutdown system which is dropping the SD2 region shown in Fig. 2-4.

McCARD calculations are conducted to verify whether the thermal spectrum core can meet the safety regulations for implementation at the KUCA. To estimate control rod worth and secondary shutdown reactivity ( $\rho_{SD2}$ ), McCARD eigenvalue calculations are performed on 500 inactive and 1,000 active cycles with 100,000 histories per cycle using ENDF/B-VIII.0 cross section libraries. To assess the excess reactivity ( $\rho_{ex}$ ), the differential reactivity and ITC, McCARD eigenvalue calculations are performed on 500 inactive and 1,000 active cycles with 1,000,000 histories per cycle. When the ambient temperature is changed from 300 K to 350 K, the inserted reactivity is calculated by a direct subtraction. In this research, the

McCARD calculations at 350 K are conducted with the continuous-energy cross section libraries produced by NJOY [11] from ENDF/B-VIII.0.

The third column in Table 2-4 shows the McCARD calculation results. The excess reactivity is about 82 pcm. The secondary shutdown reactivity is about 5,000 pcm due to the big importance of the SD2 region. From the table, one can see that the thermal spectrum core satisfies all the regulatory requirements and is found feasible with the use of the LEU modeling fuel at KUCA.

Table 2-4 Regulatory requirements of KUCA A-core and McCARD calculation results of the thermal spectrum core

Contents	Regulations for KUCA A-core	McCARD results
$\rho_{ex}$	Less than 350 pcm	$81.9 \pm 2.0$ pcm
Control rod worth	$\rho_{ex} + 1000$ pcm $\leq \sum_i^3 (C_i \text{ rod worth})$	C1 rod worth: $611 \pm 11$ pcm C2 rod worth: $235 \pm 12$ pcm C3 rod worth: $262 \pm 11$ pcm $\sum_i^3 (C_i \text{ rod worth})$ $= 1,131 \pm 11$ pcm
	$(\text{Rod worth})_{\max}$ $\leq \frac{1}{3}(\text{All rod worth})$	$\frac{1}{3}(\text{All rod worth})$ $= 754 \pm 5$ pcm
Differential reactivity	Differential reactivity at critical position $\leq 20$ pcm/s (Differential rod worth [pcm/cm] $\times$ inserted velocity [cm/s])	$11.7 \pm 0.9$ pcm/s (C1 rod)
$\rho_{SD2}$	More than 125% of $\rho_{ex}$	$5,144 \pm 12$ pcm
ITC	$\text{ITC} \leq 20$ pcm/K	$19.63 \pm 0.06$ pcm/K

Figure 2-8 shows the integral rod worth curves for the thermal spectrum core. The critical position of control rods can be estimated through the figure and  $\rho_{ex}$ . The critical position of the C1 rod, which has the largest rod worth, is 74.0 cm from the bottom. To estimate the differential rod worth at critical position, McCARD eigenvalue calculations are performed 500 inactive and 1,000 active cycles with

1,000,000 histories per cycle using ENDF/B-VIII.0 cross section libraries. When the C1 rod is axially withdrawn from 70 cm to 75 cm, the inserted reactivity is calculated by a direct subtraction. The differential C1 rod worth at critical position is  $14.6 \pm 1.0$  pcm/cm. Differential reactivity is calculated by multiplying the differential rod worth and its withdrawing velocity as much as 0.8 cm/s. The estimated differential reactivity of the C2 rod is  $11.7 \pm 0.9$  pcm/s.

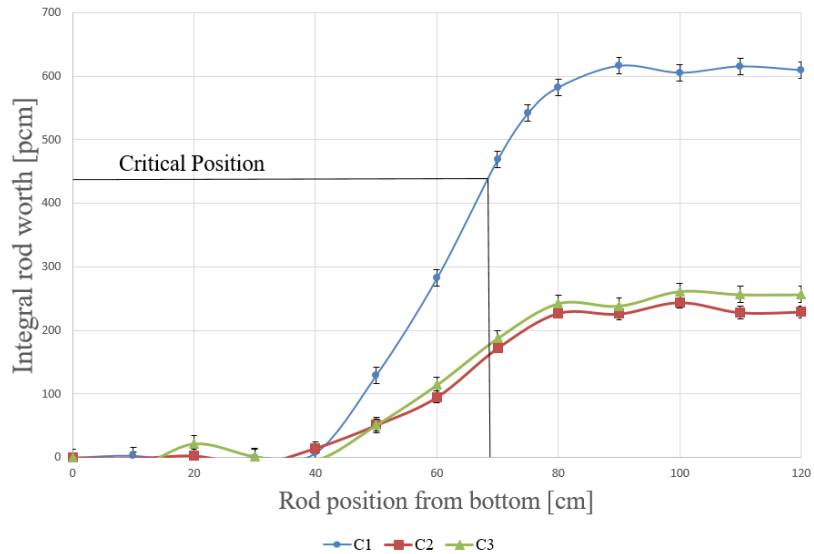


Fig. 2-8 Integral rod worth curves for the thermal spectrum core

For the water-moderated and -reflected core of KUCA, the researches on the contribution to a large positive temperature effect on reactivity [12, 13] had been conducted. In this research, the contributions of each isotope to ITC are estimated by McCARD, which has the capabilities of using the continuous-energy cross section libraries and modeling the detailed geometry.

From Table 2-4, the estimated ITC is  $19.63 \pm 0.06$  pcm/K and it is closed to the regulatory requirement of ITC. To analyze ITC, McCARD calculations for isotopic changes in microscopic cross sections are conducted for three separate regions of the core - fuel, moderator and reflector regions. The moderator region is set to PE plates used in the active core. The reflector region represents the remaining PE plates, excluding the PE used in the moderator region. It is assumed that the effects of density changes due to thermal expansion are negligible because all regions consist of solid plates. McCARD eigenvalue calculations are performed on 500 inactive and

1,000 active cycles with 100,000 histories per cycle using ENDF/B-VIII.0 cross section libraries. The contribution of each isotope to ITC is calculated by a direct subtraction between 300 K and 350 K.

Table 2-5 shows the contribution of the cross section changes of constituent isotopes in the divided regions to ITC. The ITC of each case can be obtained by summing both the region-wise and isotope-wise contributions to ITC.  $^1\text{H}_{\text{TSL}}$  indicates the thermal scattering cross section of hydrogen in PE. From the table, one can see that the Doppler-broadening effect of uranium is negligible in the ITC. It is noteworthy that the large positive contribution of  $^1\text{H}_{\text{TSL}}$  in the reflector and moderator regions is dominant. It is caused by the spectrum hardening of the thermal neutrons. The spectral shift is attributable to a decrease in the absorption reaction of hydrogen in the reflector and moderator regions. The reduction of the absorption reaction increases the effective multiplication factor.

Table 2-5 Region-wise and isotope-wise contributions of each isotope to ITC of the thermal spectrum core

Region	Isotope	Contribution of each isotope to ITC [pcm/K] (RSD [%])
Fuel	$^{234}\text{U}$	0.040 (412.3)
	$^{235}\text{U}$	0.180 (91.6)
	$^{236}\text{U}$	0.140 (117.8)
	$^{238}\text{U}$	-0.499 (33.0)
	$^{27}\text{Al}$	0.220 (75.0)
Moderator	$^1\text{H}$	-0.020 (824.6)
	$^1\text{H}_{\text{TSL}}$	9.855 (1.7)
	$^{12}\text{C}$	0.220 (75.0)
	$^{13}\text{C}$	0.020 (824.6)
Reflector	$^1\text{H}$	-0.200 (82.5)
	$^1\text{H}_{\text{TSL}}$	9.618 (1.7)
	$^{12}\text{C}$	0.000 (-)
	$^{13}\text{C}$	0.260 (63.4)
Total		19.392 (3.1)

Figure 2-9 shows the neutron spectra for the reflector and moderator regions when the ambient temperature is 300 K and 350 K, respectively. From the figure, one can see that the neutron spectra in the thermal neutron range (less than 1.0 eV) are hardened as the ambient temperature is changed from 300 K to 350 K. The average energy of thermal neutrons in the reflector region at 300 K ( $\bar{E}_{Ref}^{300K}$ ) and 350 K ( $\bar{E}_{Ref}^{350K}$ ) is changed from 6.64E-08 MeV to 7.39E-08 MeV. And, that of thermal neutrons due to the change of  $^1\text{H}_{TSL}$  in the reflector region is 7.35E-08 MeV.

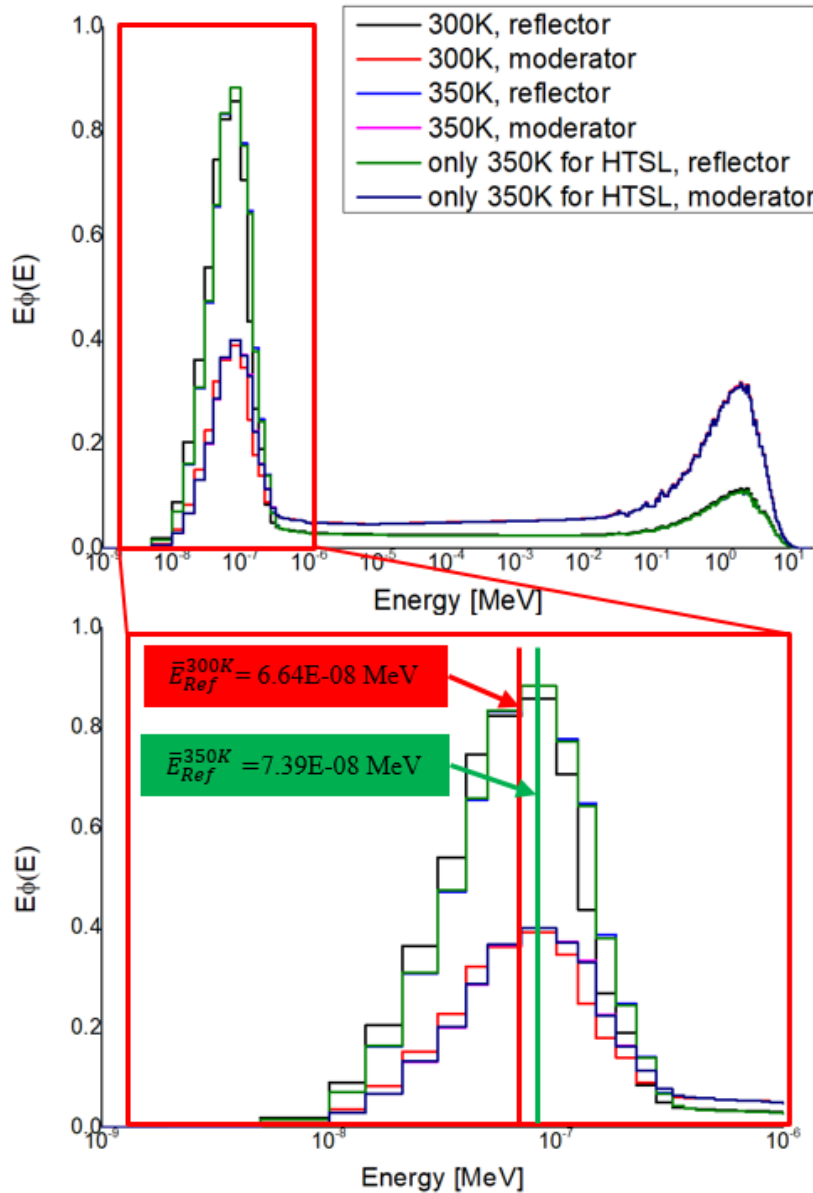


Fig. 2-9 Neutron spectra for the reflector and moderator regions of the thermal spectrum core at 300 K and 350 K

The average energy of thermal neutrons in the moderator region at 300 K ( $\bar{E}_{Mod}^{300K}$ ) and 350 K ( $\bar{E}_{Mod}^{350K}$ ) is changed from 9.64E-08 MeV to 1.03E-07 MeV. And, that of thermal neutrons due to the change of  $^1H_{TSL}$  in the moderator region is 1.03E-07 MeV.

Figure 2-10 shows the microscopic capture cross section of hydrogen. The absorption cross section of hydrogen is proportional to  $1/\sqrt{E}$ , which is proportional to  $1/v$ . The spectral shift is attributable to a decrease in the absorption reaction of hydrogen in the reflector and moderator regions. The reduction of the absorption reaction of hydrogen increases the effective multiplication factor. Therefore, the large positive ITC as much as 20 pcm/K is caused by the spectral shift effect of thermal neutrons in the reflector and moderator regions.

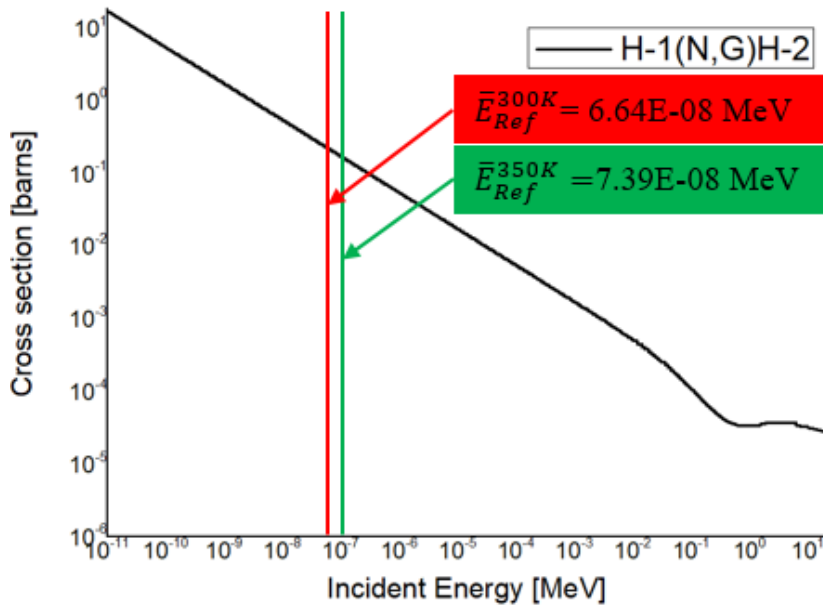


Fig. 2-10 Microscopic capture cross section of hydrogen

## 2.3 Graphite-Reflected Core

### 2.3.1 Core Description

In Chapter 2.2, the ITC of the thermal spectrum core is closed to the regulatory requirement. To reduce ITC, the graphite-reflected core is designed. The reflector element used in the fuel assembly is changed from PE to Gr as shown in Fig. 2-11.

Except for the reflector element, the Gr-reflected fuel assembly is the same as the PE-reflected one. Figure 2-12 shows the Gr-reflected thermal spectrum core comprising of 20 S14 and 3 S07 assemblies, which are shown in Appendix B. Note that 7 unit cells in S07 are determined to have the core reach its critical mass.

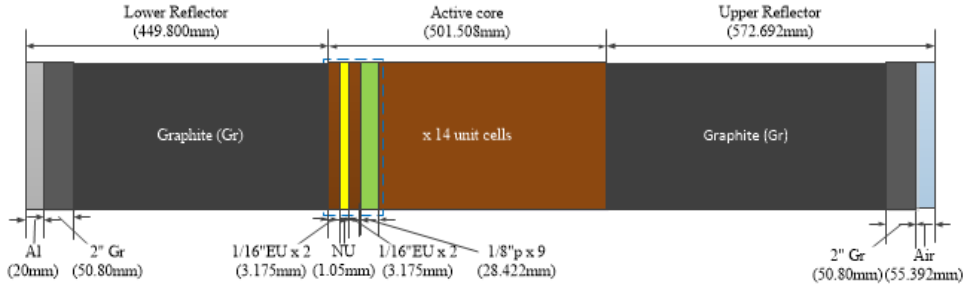


Fig. 2-11 The S14 assembly used in the Gr-reflected thermal spectrum core

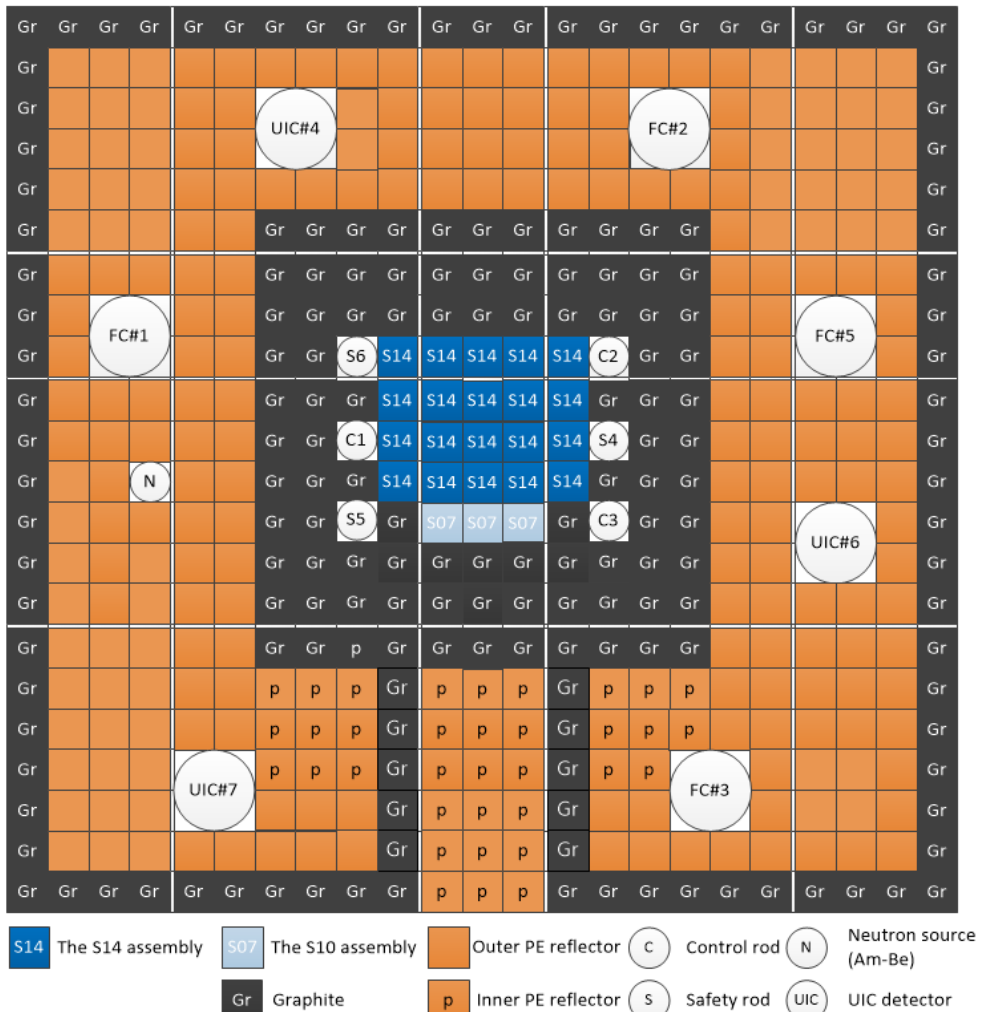


Fig. 2-12 The Gr-reflected thermal spectrum core configuration

The total number of HEU plates used in the core is 1,204 plates. The fuel assemblies are surrounded by graphite reflector elements as many as 3 layers in the radial direction.

### 2.3.2 Neutron Spectrum

To verify a thermal spectrum in the core, one representative position to check the neutron energy spectrum is chosen as shown on the left side of Fig. 2-13. Also, the spectrum of the core is compared with that of the PE-reflected thermal spectrum core as shown on the right side of Fig. 2-13. In the MC eigenvalue calculations, neutron spectra are tallied for two unit cells located in the middle height of each fuel assembly position. Figure 2-14 shows comparisons of each regional spectrum.

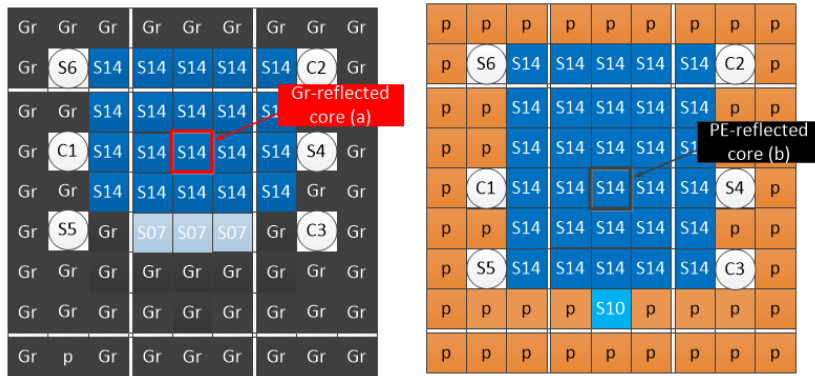


Fig. 2-13 Tally positions for neutron energy spectrum analyses (Left: the Gr-reflected core, Right: the PE-reflected core)

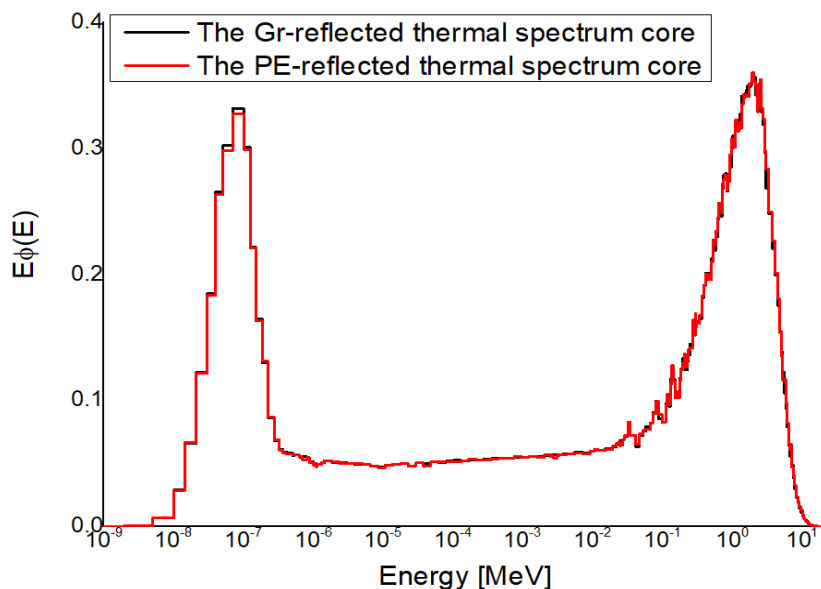


Fig. 2-14 Neutron spectra for (a) the Gr-reflected core, (b) the PE-reflected core

### 2.3.3 Neutronics Parameters

McCARD calculations are conducted to verify whether the Gr-reflected thermal spectrum core can meet the safety regulations for implementation at the KUCA. To estimate the excess reactivity ( $\rho_{ex}$ ), control rod worth and secondary shutdown reactivity ( $\rho_{SD2}$ ), McCARD eigenvalue calculations are performed on 500 inactive and 1,000 active cycles with 100,000 histories per cycle using ENDF/B-VIII.0 cross section libraries. To assess the differential reactivity and ITC, McCARD eigenvalue calculations are performed on 500 inactive and 1,000 active cycles with 1,000,000 histories per cycle. When the ambient temperature is changed from 300 K to 350 K, the inserted reactivity is calculated by a direct subtraction.

Table 2-6 Regulatory requirements of KUCA A-core and McCARD calculation results of the Gr-reflected thermal spectrum core

Contents	Regulations for KUCA A-core	McCARD results
$\rho_{ex}$	Less than 350 pcm	240.4±8.0 pcm
Control rod worth	$\rho_{ex} + 1000 \text{ pcm}$ $\leq \sum_i^3 (C_i \text{ rod worth})$	C1 rod worth: 1,264±11 pcm C2 rod worth: 1,005±11 pcm C3 rod worth: 840±11 pcm $\sum_i^3 (C_i \text{ rod worth})$ =3,109±20 pcm
	$(\text{Rod worth})_{\max}$ $\leq \frac{1}{3}(\text{All rod worth})$	$\frac{1}{3}(\text{All rod worth})$ =2,073±9 pcm
Differential reactivity	Differential reactivity at critical position $\leq 20 \text{ pcm/s}$ (Differential rod worth [pcm/cm] ×inserted velocity [cm/s])	13.9±0.5 pcm/s (C1 rod)
$\rho_{SD2}$	More than 125% of $\rho_{ex}$	10,845±13 pcm
ITC	ITC $\leq 20 \text{ pcm/K}$	13.48±0.25 pcm/K

The third column in Table 2-6 shows the McCARD calculation results. The excess reactivity is about 240 pcm. The secondary shutdown reactivity is about

11,000 pcm due to the big importance of the center region. From the table, one can see that the Gr-reflected hybrid spectrum core satisfies all the regulatory requirements.

Figure 2-15 shows the integral rod worth curves for the Gr-reflected thermal spectrum core. The critical position of control rods can be estimated through the figure and  $\rho_{ex}$ . The critical position of the C1 rod, which has the largest rod worth, is 75.1 cm from the bottom. To estimate the differential rod worth at critical position, McCARD eigenvalue calculations are performed 500 inactive and 1,000 active cycles with 1,000,000 histories per cycle using ENDF/B-VIII.0 cross section libraries. When the C1 rod is axially withdrawn from 75 cm to 80 cm, the inserted reactivity is conservatively calculated by a direct subtraction. The differential C1 rod worth at critical position is  $17.4 \pm 0.6$  pcm/cm. Differential reactivity is calculated by multiplying the differential rod worth and its withdrawing velocity as much as 0.8 cm/s. The estimated differential reactivity of the C2 rod is  $13.9 \pm 0.5$  pcm/s.

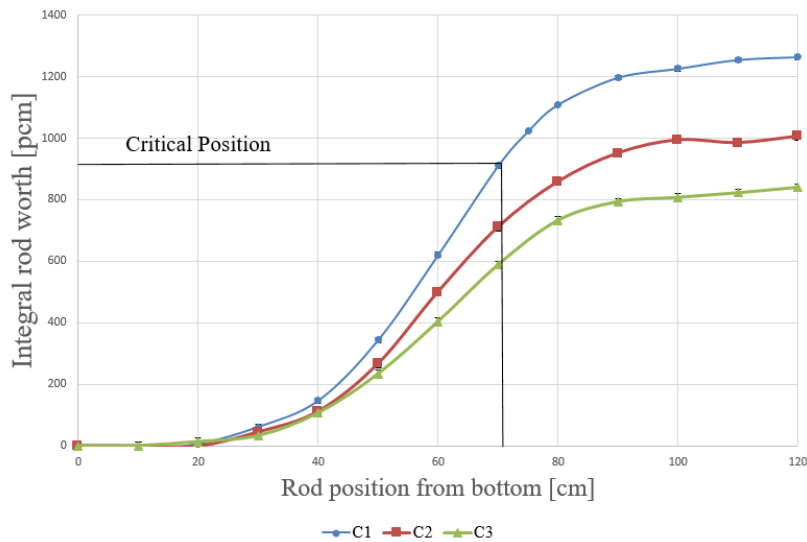


Fig. 2-15 Integral rod worth curves for the Gr-reflected thermal spectrum core

From Table 2-6, the estimated ITC is  $13.38 \pm 0.25$  pcm/K. To analyze ITC, McCARD calculations for isotopic changes in thermal scattering cross section are conducted for the reflector and moderator regions of the core. McCARD eigenvalue calculations are performed on 500 inactive and 1,000 active cycles with 100,000 histories per cycle using ENDF/B-VIII.0 cross section libraries. The contribution of

the thermal scattering cross section of hydrogen ( $^1\text{H}_{\text{TSL}}$ ) to ITC is calculated by a direct subtraction between 300 K and 350 K while that of graphite ( $\text{C}_{\text{TSL}}$ ) to ITC is calculated by a direct subtraction between 296 K and 400 K.

Table 2-7 shows the contribution of the thermal scattering cross section changes of isotopes. From the table, one can see that the ITC of the core can be obtained by summing the contributions of the thermal scattering cross section. The contribution of the thermal scattering cross section change of hydrogen in the reflector region decreases from 9.6 pcm/K to 2.0 pcm/K by varying the reflector element from PE to Gr. However, the contribution of thermal scattering cross section of hydrogen in the moderator region is still dominant because of the 9 PE plates used in the LEU modeling unit cell. Compared with the contribution of  $^1\text{H}_{\text{TSL}}$  in the reflector region, that of  $\text{C}_{\text{TSL}}$  to ITC is minor due to the small absorption cross section of carbon.

Table 2-7 Region-wise contribution of thermal scattering cross section to ITC of the thermal spectrum core

Region	Isotope	Contribution of each isotope to ITC [pcm/K] (RSD [%])	
		The Gr-reflected core	The PE-reflected core
Moderator	$^1\text{H}_{\text{TSL}}$	10.572 (2.1)	9.855 (1.7)
Reflector	$^1\text{H}_{\text{TSL}}$	2.028 (11.1)	9.618 (1.7)
	$\text{C}_{\text{TSL}}$	0.794 (13.6)	0.000 (-)
Total		13.394 (2.5)	19.473 (1.2)
ITC		13.483 (1.9)	19.633 (0.3)

Figure 2-16 shows the neutron spectra for the reflector and moderator regions when the ambient temperature is 300 K and 350 K. From the figure, one can see that the neutron spectra in the thermal neutron range (less than 1.0 eV) are hardened as the ambient temperature is changed from 300 K to 350 K. Without considering the change of  $\text{C}_{\text{TSL}}$ , the average energy of thermal neutrons in the reflector region at 300 K and 350 K is changed from  $8.04\text{E-}08$  MeV to  $8.35\text{E-}08$  MeV. And, that of thermal neutrons due to the change of  $^1\text{H}_{\text{TSL}}$  in the reflector region is  $8.34\text{E-}08$  MeV. The average thermal neutron energy in the reflector region of the Gr-reflected core is less hardened by 59 % than that of the PE-reflected one. The average energy of thermal neutrons in the reflector region of thermal neutrons due to the change of  $\text{C}_{\text{TSL}}$  from

296 K to 400 K is  $8.83\text{E-}08$  MeV. The average energy of thermal neutrons in the moderator region is changed from  $9.89\text{E-}08$  MeV to  $1.05\text{E-}07$  MeV. And, that of thermal neutrons due to the change of  $^1\text{H}_{\text{TSL}}$  in the moderator region is  $1.05\text{E-}07$  MeV.

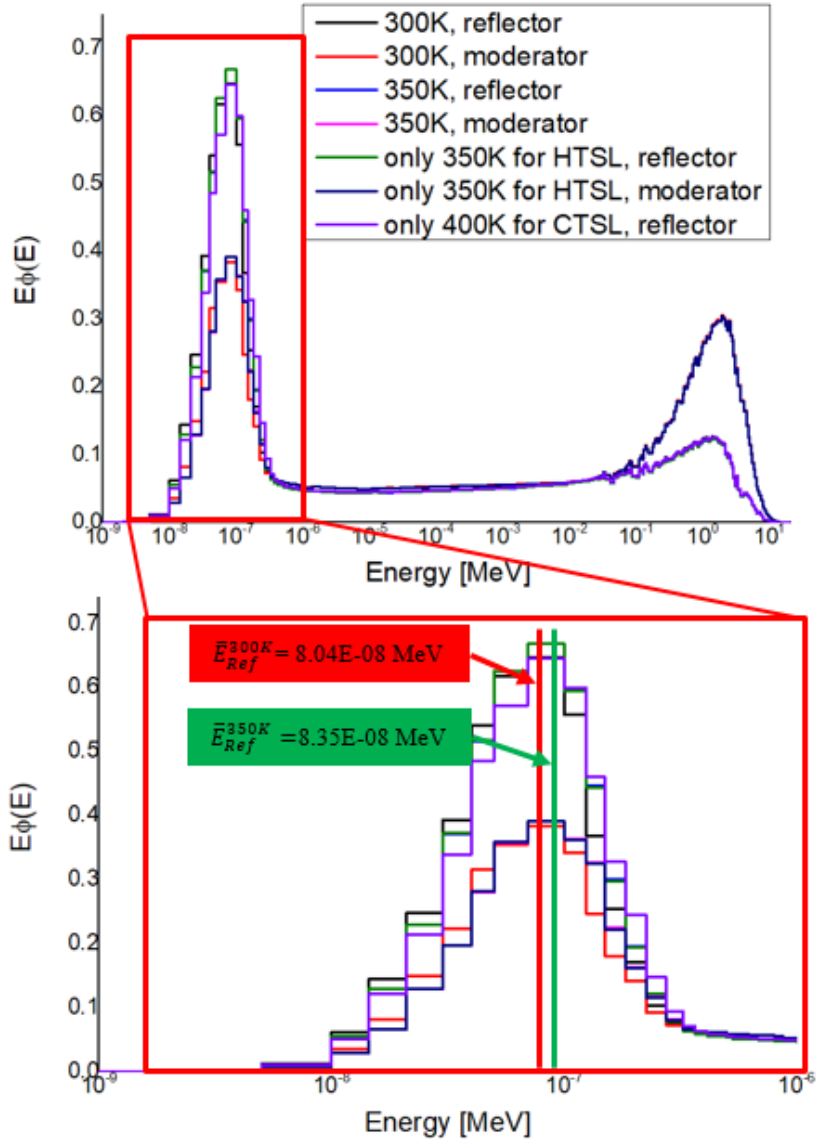


Fig. 2-16 Neutron spectra for the reflector and moderator regions of the Gr-reflected thermal spectrum core at 300 K and 350 K

Figure 2-17 shows the microscopic capture cross sections of hydrogen and carbon. The absorption cross sections of hydrogen and carbon are proportional to  $1/v$ . The spectral shift of thermal neutrons in the reflector region is attributable to a

decrease in the absorption reactions of carbon and hydrogen. The reduction of the absorption reaction increases the effective multiplication factor. Therefore, the contribution of the reflector element to the ITC are positive.

By varying the reflector element from PE to Gr, the contribution of the reflector element in the Gr-reflected core is reduced about 3.4 times despite the positive contribution of  $C_{TSL}$  to the ITC. From the figure, one can see that the capture cross section of hydrogen is 100 times larger than that of carbon in the thermal neutron range. The inserted positive reactivity due to a decrease in the absorption reaction in the reflector region is reduced when the reflector element is changed from PE to Gr. Therefore, the contribution of the reflector element decreases from 9.6 pcm/K to 2.0 pcm/K due to the small absorption cross sections of  $^{12}\text{C}$  and  $^{13}\text{C}$ . With these results, one can see that Gr is an appropriate reflector element to reduce ITC.

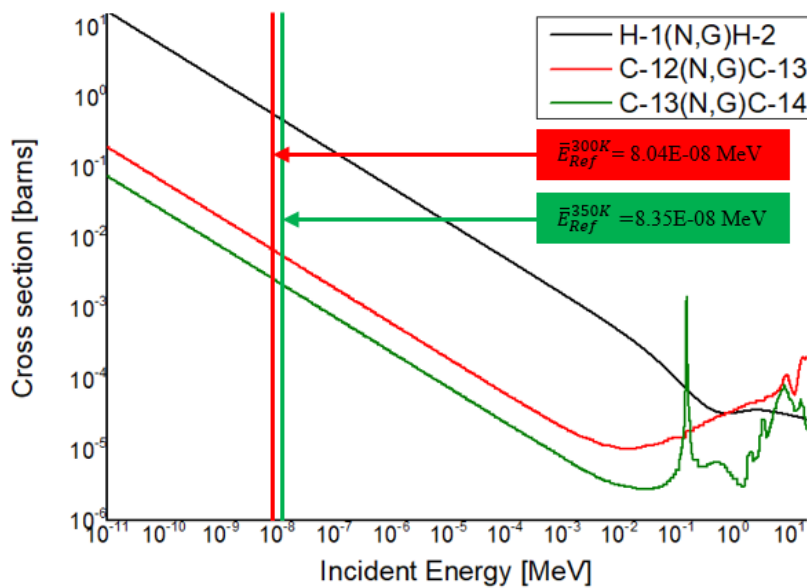


Fig. 2-17 Microscopic capture cross section of hydrogen and carbon

# Chapter 3. Fast-Thermal Hybrid Spectrum Core Design

## 3.1 Low-Enriched Uranium Modeling Fuel

To make a core with a fast spectrum, the LEU modeling unit cell is designed without the PE plates as a moderator. The LEU modeling unit cell is composed of four HEU plates and one NU plate (1/16"HEU×2+1.05 mm thick NU+1/16"HEU×2) as shown in Fig. 2-1 (Chapter 2.1).

To determine the number of the LEU modeling unit cells in the test assembly (T), the criticality of the test assembly is estimated by varying the number of the LEU modeling unit cells while fixing the center position of the active core to 69.9 cm from the bottom. The MC  $k$ -eigenvalue calculations are conducted for seven test assemblies, increasing the number of the unit cells stacked in the test assembly from 20 to 44 in multiples of 4 (T20, T24, T28, T32, T36, T40 and T44). McCARD calculations are performed on 500 inactive and 1,000 active cycles with 100,000 histories per cycle using ENDF/B-VIII.0 cross section libraries. Figure 3-1 shows the infinite multiplication factor ( $k_{inf}$ ) for the single assembly with reflective boundary conditions.

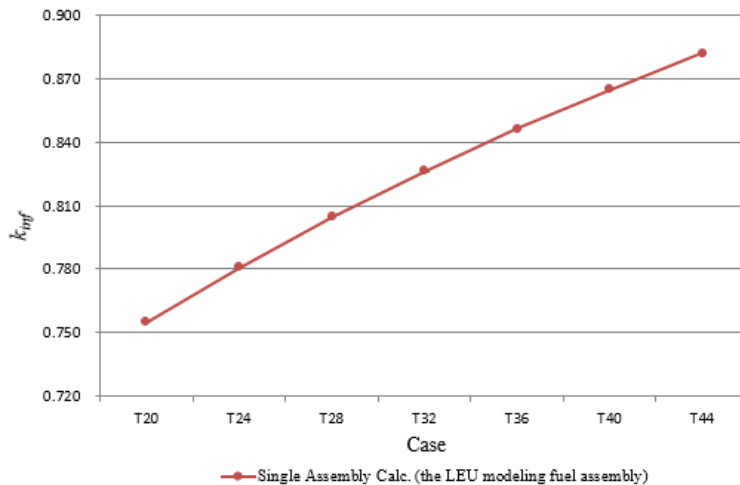


Fig. 3-1  $k_{inf}$  sensitivities of the number of LEU modeling unit cells stacked in the test assembly

From the figure, one can see that the infinite multiplication factor increases as the number of unit cells increases but the LEU modeling fuel assembly could not reach the criticality regardless of the number of unit cells because the moderator plate is not used in the unit cell. From these results, it can be seen that the fast spectrum core with the only LEU modeling fuel assemblies is hard to reach criticality.

To design a core with a fast spectrum region using the test assembly, the preliminary hybrid spectrum core is introduced. Figure 3-2 shows the preliminary hybrid spectrum core to determine the number of the LEU modeling unit cells stacked in the assembly.

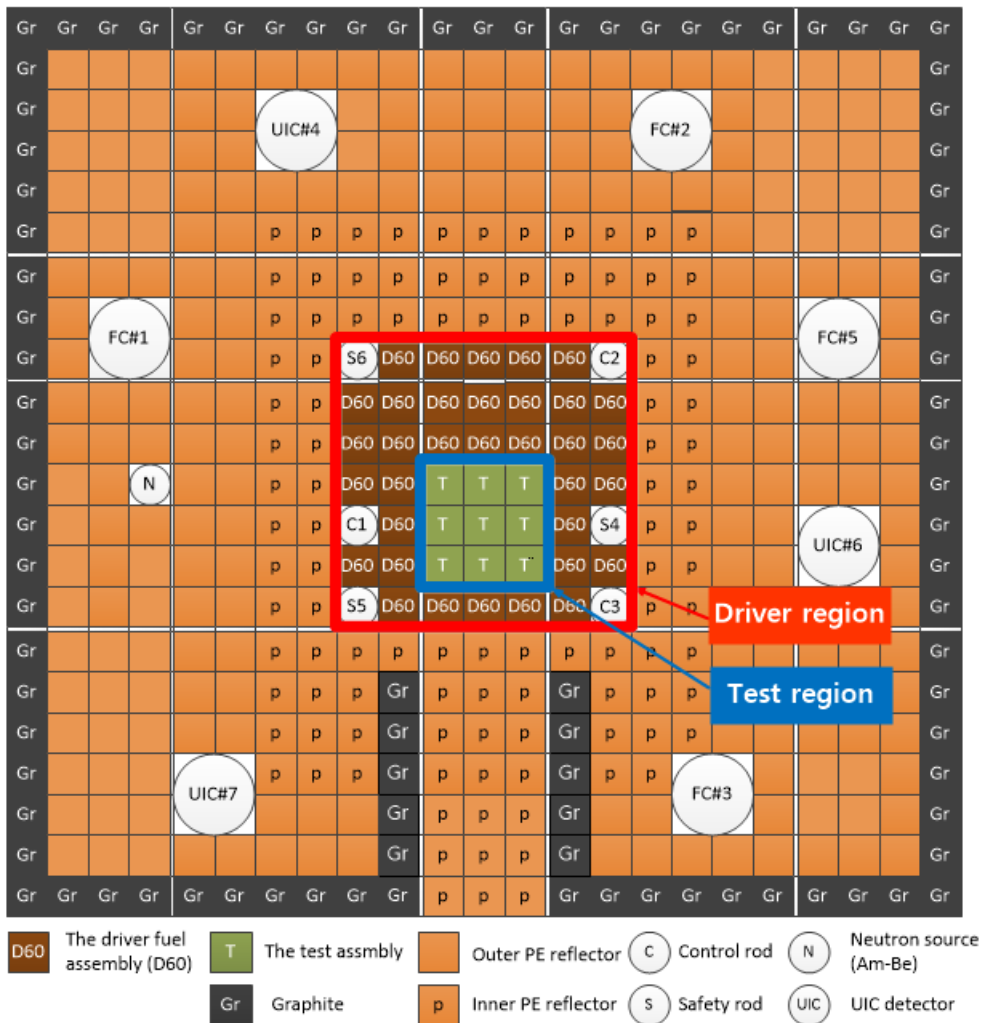


Fig. 3-2 The preliminary hybrid spectrum core configuration (Red line: the driver region, Blue line: the test region)

The hybrid spectrum core is designed to have two regions - a driver region comprising the driver fuel assemblies (D60; Fig. 2-6) and a test region using the test assemblies (T) because the core composed only of the test assemblies is difficult to reach criticality. The infinite multiplication factor for the single D60 assembly with reflective boundary conditions is  $1.45941 \pm 0.00005$ .

To determine the number of unit cells in the LEU modeling fuel assembly, the effective multiplication factor ( $k_{eff}$ ) of the preliminary hybrid spectrum core is estimated by varying the number of the LEU modeling unit cells. The MC  $k$ -eigenvalue calculations are conducted for seven test assemblies which are T20, T24, T28, T32, T36, T40 and T44. McCARD calculations are performed on 500 inactive and 1,000 active cycles with 100,000 histories per cycle using ENDF/B-VIII.0 cross section libraries. Figure 3-3 shows the effective multiplication factor ( $k_{eff}$ ) for the preliminary core according to the number of the LEU modeling unit cells. The number of unit cells in T is determined to have the largest effective multiplication factor of the hybrid spectrum core.

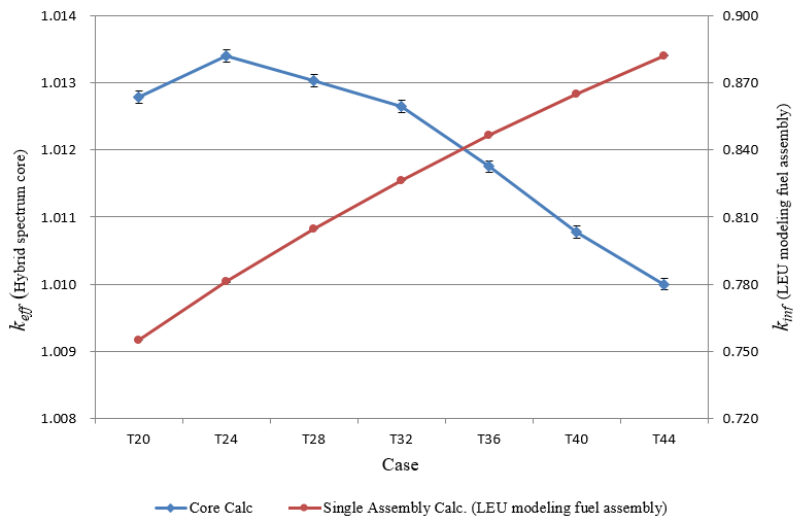


Fig. 3-3  $k$  sensitivities of the number of LEU modeling unit cells stacked in the LEU modeling fuel assembly

For the preliminary core, it has the largest value of  $k_{eff}$  when 24 unit cells are used in the LEU modeling fuel assembly. Unlike the trend of the single assembly calculations, the trend of  $k_{eff}$  decreases as the number of unit cells increases from 24

unit cells because the upper and lower reflector regions comprising PE plates, which also play a role of moderator, in the LEU modeling fuel assembly decreases axially as the number of the LEU modeling unit cells increases. Since the importance of the D60 assemblies in the driver region is much greater than that of the LEU modeling fuel assemblies in the test region,  $k_{eff}$  decreases as the reflector regions comprising the PE plates in the test assembly decrease. According to the results, the number of unit cells stacked in the LEU modeling fuel assembly is determined to 24.

Twenty-four LEU modeling unit cells are stacked in the test assembly (T24), which is the LEU modeling fuel assembly. The total length of its active core region is about 18 cm. The lower and upper reflectors are composed of polyethylene (PE) plates. Figures 3-4 and 3-5 show the T24 assembly and its active core region, respectively.

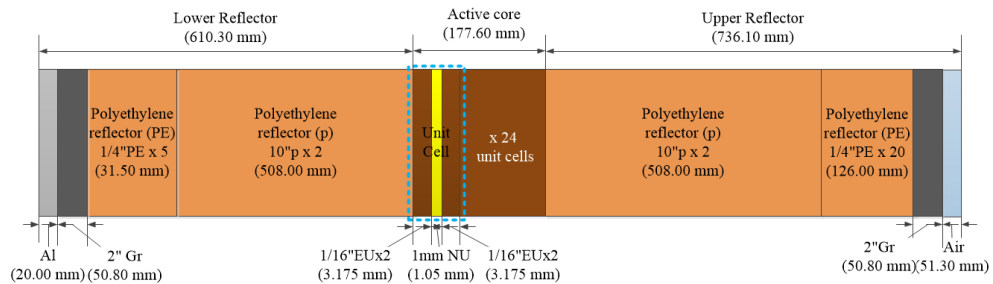


Fig. 3-4 The T24 assembly used in the fast-thermal hybrid spectrum core

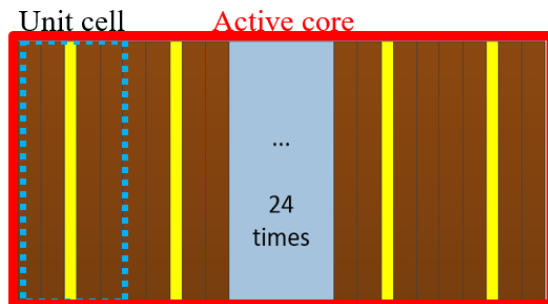


Fig. 3-5 The active core region in T24

## 3.2 Polyethylene-Moderated Core

### 3.2.1 Core Description

The designed hybrid spectrum core has two different regions as shown in Fig.

3-6. The test region is composed of 9 T24 assemblies and the driver region consists of 31 D60 and 3 D04 assemblies. In the D04 assembly, the fuel unit cells composed of two 3.175 mm (1/8”) thick HEU plates and a 3.158 mm (1/8”) thick polyethylene plate are stacked as many as 4. Note that 4 unit cells in D04 are determined to have the core reach its critical mass. The black area called the SD2 region is a secondary shutdown system. The total number of HEU plates used in the core is 4,608 plates.

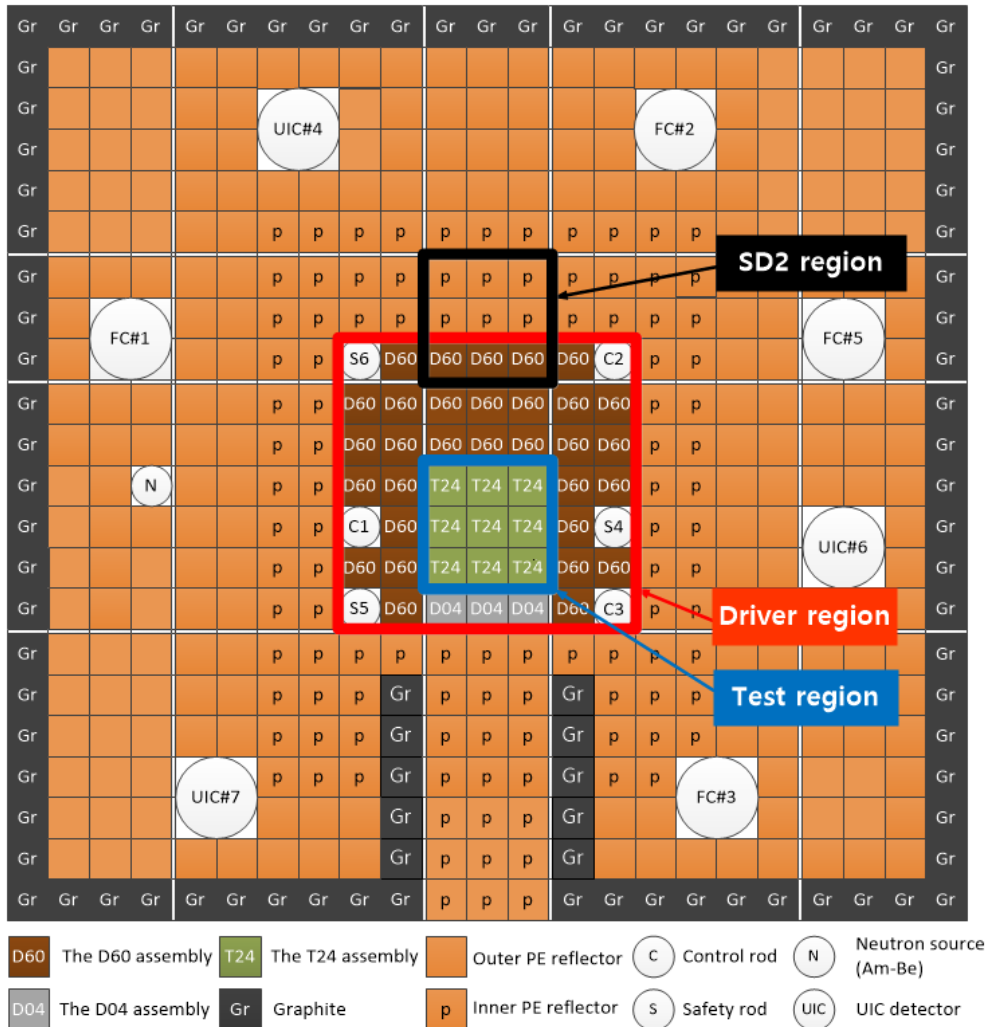


Fig. 3-6 Hybrid spectrum core configuration

### 3.2.2 Neutron Spectrum

To verify a hard spectrum in the test region, three representative positions to check their neutron energy spectra are chosen as shown on the left side of Fig. 3-7 –

(a) upper driver region, (b) test region and (c) lower driver region. Also, the spectrum of the hybrid spectrum core is compared with that of the thermal spectrum core (d). In the MC eigenvalue calculations, neutron spectra are tallied for two unit cells located in the middle height of each fuel assembly position. Figure 3-8 shows comparisons of each regional spectrum. From the figure, one can see that a fast spectrum can be obtained in the test region because the PE plates are not used in the fuel unit cells of T24.

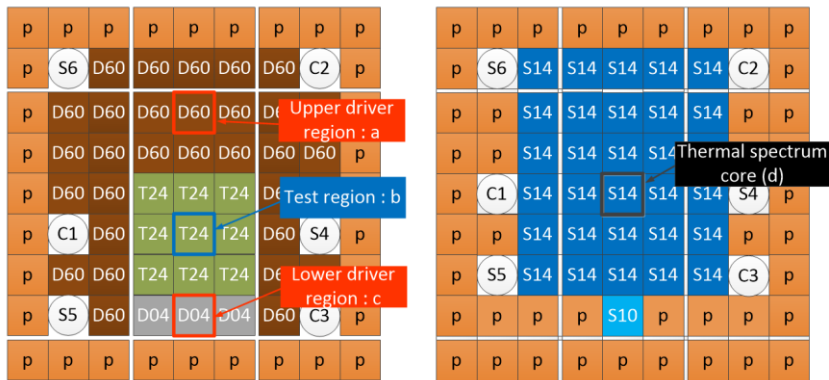


Fig. 3-7 Tally positions for neutron energy spectrum analyses (Left: the hybrid spectrum core, Right: the thermal spectrum core)

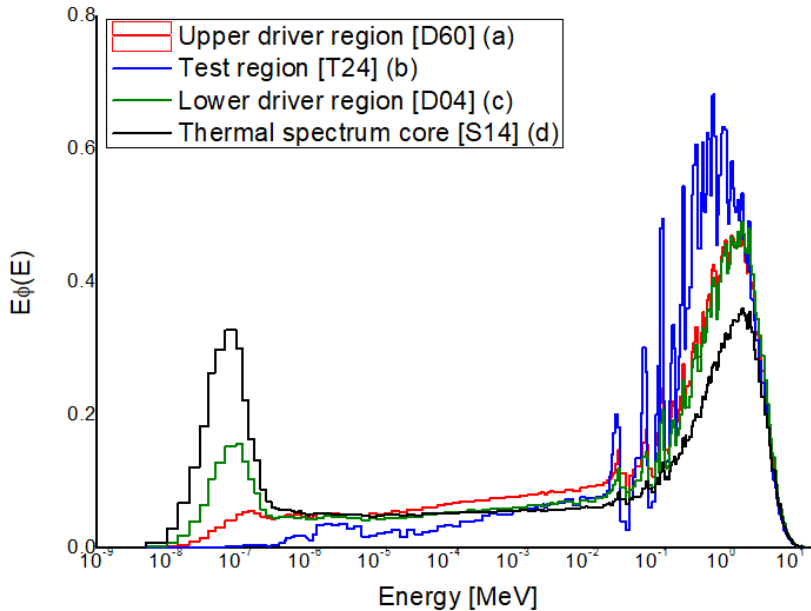


Fig. 3-8 Neutron spectra for (a) upper driver region, (b) test region, (c) lower driver region and (d) the thermal spectrum core

### 3.2.3 Neutronics Parameters

McCARD calculations are conducted to verify whether the hybrid spectrum core can meet the safety regulations for implementation at the KUCA. To estimate the excess reactivity ( $\rho_{ex}$ ), control rod worth and secondary shutdown reactivity ( $\rho_{SD2}$ ), McCARD eigenvalue calculations are performed on 500 inactive and 1,000 active cycles with 100,000 histories per cycle using ENDF/B-VIII.0 cross section libraries. To assess the differential reactivity and the isothermal temperature coefficient (ITC), McCARD eigenvalue calculations are performed on 500 inactive and 1,000 active cycles with 1,000,000 histories per cycle. When the ambient temperature is changed from 300 K to 350 K, the inserted reactivity is calculated by a direct subtraction. The third column in Table 3-1 shows the McCARD calculation results.

Table 3-1 Regulatory requirements of KUCA A-core and McCARD calculation results of the hybrid spectrum core

Contents	Regulations for KUCA A-core	McCARD results
$\rho_{ex}$	Less than 350 pcm	133.8±9.0 pcm
Control rod worth	$\rho_{ex} + 1000 \text{ pcm}$ $\leq \sum_i^3 (C_i \text{ rod worth})$	C1 rod worth: 809±13 pcm C2 rod worth: 831±13 pcm C3 rod worth: 277±13 pcm $\sum_i^3 (C_i \text{ rod worth})$ =1,917±22 pcm
	$(\text{Rod worth})_{\max}$ $\leq \frac{1}{3}(\text{All rod worth})$	$\frac{1}{3}(\text{All rod worth})$ =1,278±10 pcm
Differential reactivity	Differential reactivity at critical position $\leq 20 \text{ pcm/s}$ (Differential rod worth [pcm/cm] ×inserted velocity [cm/s])	15.36±0.97 pcm/s (C2 rod)
$\rho_{SD2}$	More than 125% of $\rho_{ex}$	9,427±14 pcm
ITC	ITC $\leq 20 \text{ pcm/K}$	19.79±0.08 pcm/K

The excess reactivity is about 130 pcm. It is noteworthy that the C1 rod worth is smaller than C2 rod worth because the importance of its circumjacent test region is relatively smaller than that of C2. The secondary shutdown reactivity is about 9,500 pcm which is about 2 times larger than that of the thermal spectrum core due to the big importance of the SD2 region. From the table, one can see that the hybrid spectrum core satisfies all the regulatory requirements except ITC considering its 95% confidence intervals.

Figure 3-9 shows the integral rod worth curves for the hybrid spectrum core. The critical position of control rods can be estimated through the figure and excess reactivity. The critical position of the C2 rod, which has the largest rod worth, is 72.4 cm from the bottom. To estimate the differential rod worth at critical position, McCARD eigenvalue calculations are performed 500 inactive and 1,000 active cycles with 1,000,000 histories per cycle using ENDF/B-VIII.0 cross section libraries. When the C2 rod is axially withdrawn from 70 cm to 75 cm, the inserted reactivity is calculated by a direct subtraction. The differential C2 rod worth at critical position is  $19.2 \pm 1.2$  pcm/cm. Differential reactivity is calculated by multiplying the differential rod worth and its withdrawing velocity as much as 0.8 cm/s. The estimated differential reactivity of the C2 rod is  $15.3 \pm 1.0$  pcm/s.

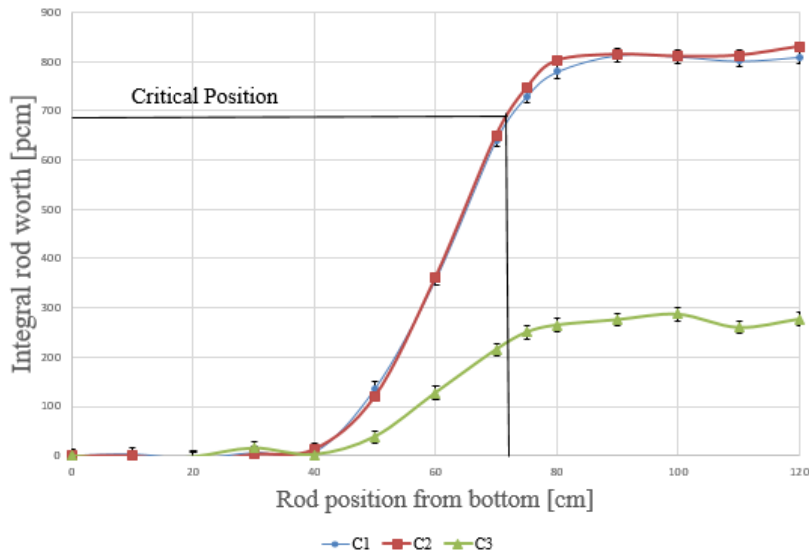


Fig. 3-9 Integral rod worth curves of the hybrid spectrum core

From Table 3-1, one can see that the hybrid spectrum core satisfies the regulatory requirement of ITC considering its 95% confidence intervals. To analyze ITC, McCARD calculations for isotopic changes in microscopic cross sections are conducted for three separate regions of the core – fuel, moderator and reflector regions. The moderator region is set to PE plates used in the active core. The reflector region represents the remaining PE plates, excluding the PE used in the moderator region. It is assumed that the effects of density changes due to thermal expansion are negligible because all regions consist of solid plates. McCARD eigenvalue calculations are performed on 500 inactive and 1,000 active cycles with 1,000,000 histories per cycle using ENDF/B-VIII.0 cross section libraries. The contribution of each isotope to ITC is calculated by a direct subtraction between 300 K and 350 K. Table 3-2 shows the contribution of the cross section changes of constituent isotopes in the divided regions to the ITC. Note that the ITC of each case can be obtained by summing up all the region-wise and isotope-wise contribution to ITC.

Table 3-2 Region-wise and isotope-wise contribution of each isotope to ITC of the hybrid spectrum core

Region	Isotope	Contribution of each isotope to ITC [pcm/K] (RSD [%])
Fuel	<sup>234</sup> U	0.020 (424.3)
	<sup>235</sup> U	-0.219 (38.6)
	<sup>236</sup> U	0.040 (212.1)
	<sup>238</sup> U	-0.180 (47.1)
	<sup>27</sup> Al	0.000 (-)
Moderator	<sup>1</sup> H	-0.080 (106.1)
	<sup>1</sup> H <sub>TSL</sub>	-1.757 (4.8)
	<sup>12</sup> C	0.100 (84.9)
	<sup>13</sup> C	0.060 (141.4)
Reflector	<sup>1</sup> H	0.020 (424.3)
	<sup>1</sup> H <sub>TSL</sub>	21.294 (0.4)
	<sup>12</sup> C	0.140 (60.6)
	<sup>13</sup> C	0.020 (424.3)
Total		19.457 (1.6)

From the table, one can see that the Doppler-broadening effect of uranium is negligible in the ITC. It is noteworthy that the positive contribution of the thermal scattering cross section change of hydrogen in the reflector region is dominant. It is caused by the spectrum hardening of the thermal neutrons. The spectral shift is attributable to a decrease in the absorption reaction of hydrogen in the reflector region. The reduction of the absorption reaction increases the effective multiplication factor. Figure 3-10 shows the neutron spectra for the reflector and moderator regions when the ambient temperature is 300 K and 350 K.

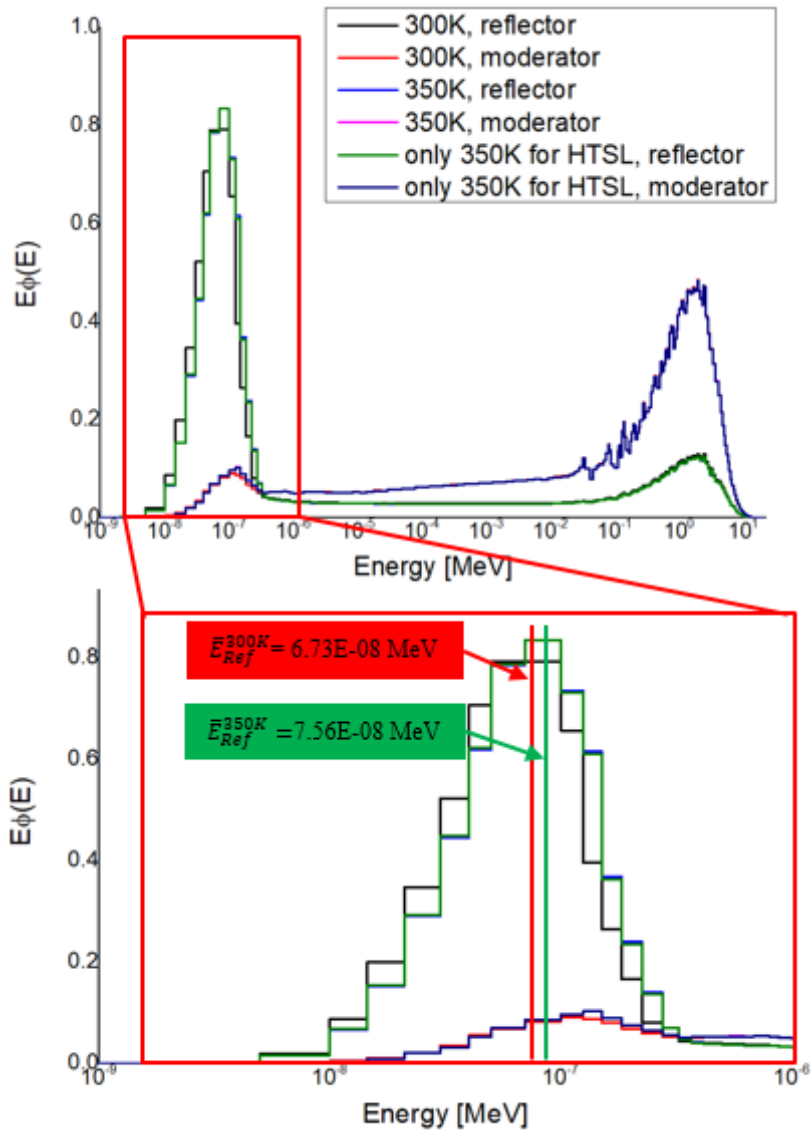


Fig. 3-10 Neutron spectra for the reflector and moderator regions of the hybrid spectrum core at 300 K and 350 K

From the figure, one can see that the neutron spectra in the thermal neutron range (less than 1.0 eV) are hardened as the ambient temperature is changed from 300 K to 350 K. The average energy of thermal neutrons in the reflector region at 300 K and 350 K is changed from 6.73E-08 MeV to 7.56E-08 MeV. And, that of thermal neutrons due to the change of  $^1\text{H}_{\text{TSL}}$  in the reflector region is 7.53E-08 MeV. The average energy of thermal neutrons in the moderator region is changed from 1.98E-07 MeV to 1.99E-07 MeV. And, that of thermal neutrons due to the change of  $^1\text{H}_{\text{TSL}}$  in the moderator region is 1.99E-07 MeV.

The absorption cross section of hydrogen is proportional to  $1/v$ . The thermal spectrum hardening in the moderator region decreases not only the absorption reaction of hydrogen in the moderator region but the fission reaction in the fuel region. The reduction of the fission reaction decreases the effective multiplication factor. The contribution of the decrease in the fission reaction to ITC is more dominant than that in the absorption reaction to ITC because of the relatively small number of the PE plates used in the moderator region. Therefore, the total contribution of the spectral shift effect in the moderator region to the ITC is negative.

The spectral shift is attributable to a decrease in the absorption reaction of hydrogen in the reflector region. The reduction of the absorption reaction increases the effective multiplication factor. Therefore, the contribution in the reflector region to the ITC is positive. The average thermal neutron energy in the moderator region is hardly hardened than that in the reflector region because of the relatively small number of the PE plates used in the moderator region. The contribution of the reflector element to ITC is much more dominant than that of the moderator element. Therefore, the large ITC as much as 20 pcm/K of the hybrid spectrum core is caused by the effect of the spectral shift of thermal neutrons in the reflector region.

### **3.3 Graphite-Reflected Core**

#### **3.3.1 Core Description**

In Chapter 3.2.3, the ITC of the hybrid spectrum core is closed to the regulatory requirement. To reduce ITC, the graphite-reflected core is designed as shown in Fig. 3-11. The reflector element used in the fuel assembly is changed from PE to Gr.

Except for the reflector element, the Gr-reflected fuel assembly is the same as the PE-reflected one.

The test region is composed of 9 T24 assemblies and the driver region in the core consists of 21 D60 and one D20 assemblies. Figures 3-12 and 3-13 show the Gr-reflected D60 and T24 assemblies, respectively. Note that 20 unit cells stacked in D20 are determined to have the core reach its critical mass. The total number of HEU plates used in the core is 3,424 plates. The driver region is surrounded by graphite reflector elements as many as 3 layers in the radial direction.

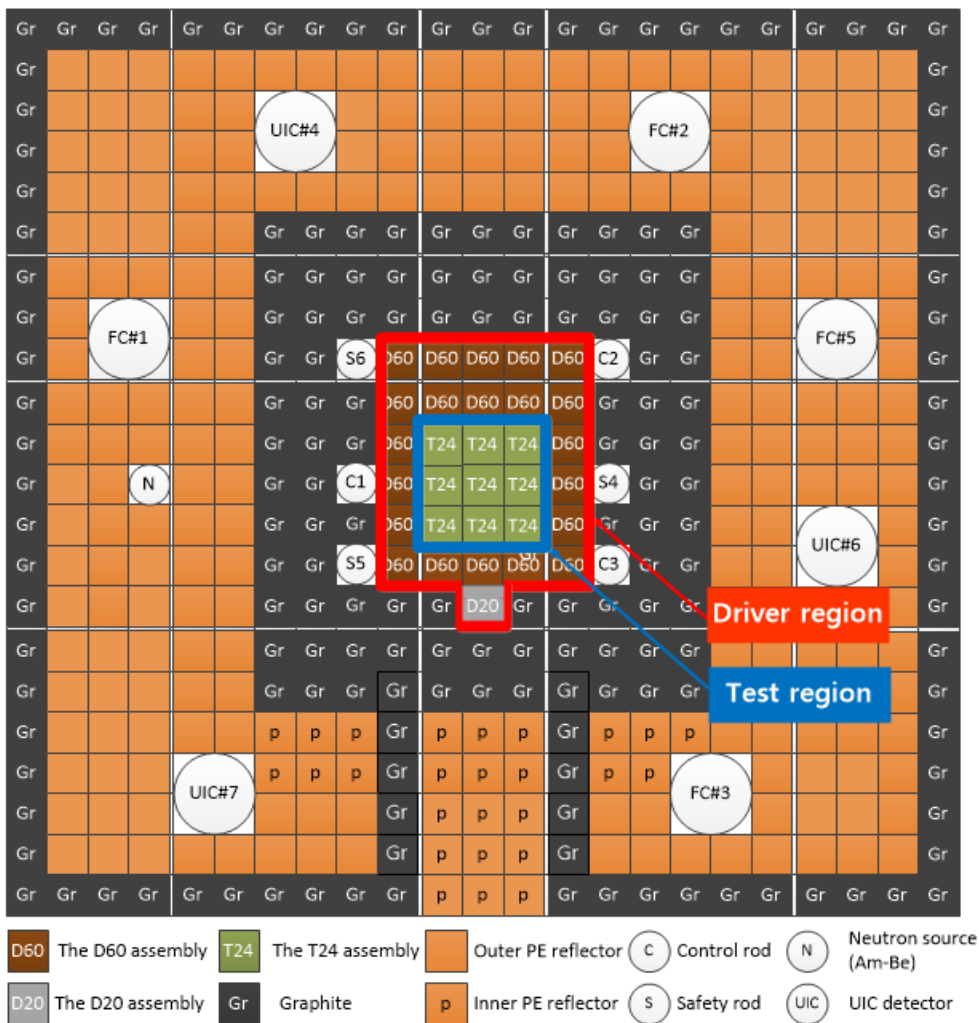


Fig. 3-11 The Gr-reflected hybrid spectrum core configuration

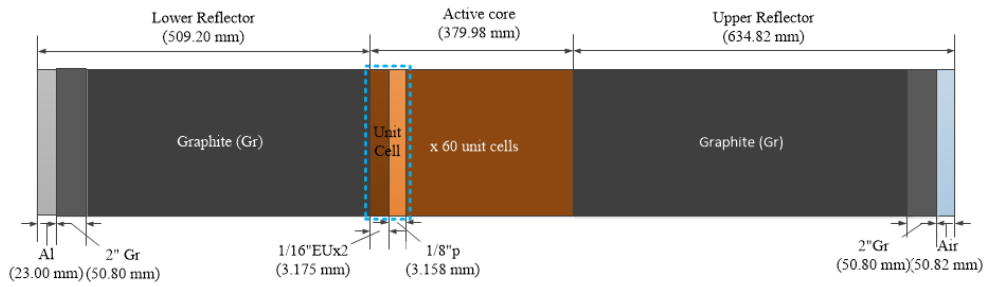


Fig. 3-12 The D60 assembly used in the Gr-reflected hybrid spectrum core

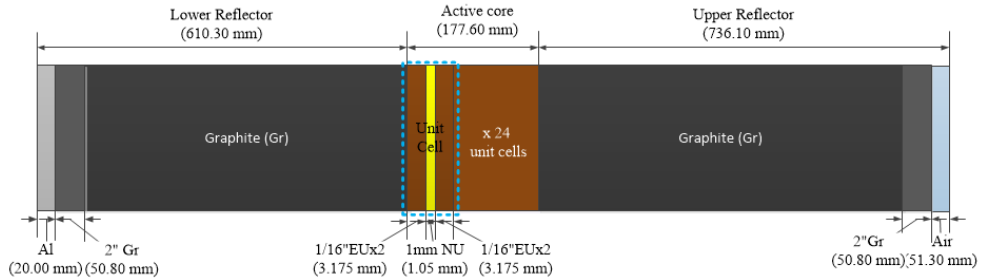


Fig. 3-13 The T24 assembly used in the Gr-reflected hybrid spectrum core

### 3.3.2 Neutron Spectrum

To verify a hard spectrum in the test region, three representative positions to check their neutron energy spectrum are chosen as shown on the left side of Fig. 3-14 – (a) upper driver region, (b) test region and (c) lower driver region. Also, the spectra are compared with that of the test region (d) of the PE-moderated hybrid spectrum core as shown on the right side of Fig. 3-14.



Fig. 3-14 Tally positions for neutron energy spectrum analyses (Left: the Gr-reflected core, Right: the PE-moderated core)

In the MC eigenvalue calculations, neutron spectra are tallied for two unit cells located in the middle height of each fuel assembly position. Figure 3-15 shows comparisons of each regional spectrum. From the figure, one can see that a fast spectrum can be obtained in the test region of two cores because the PE plates are not used in the fuel unit cells of T24.

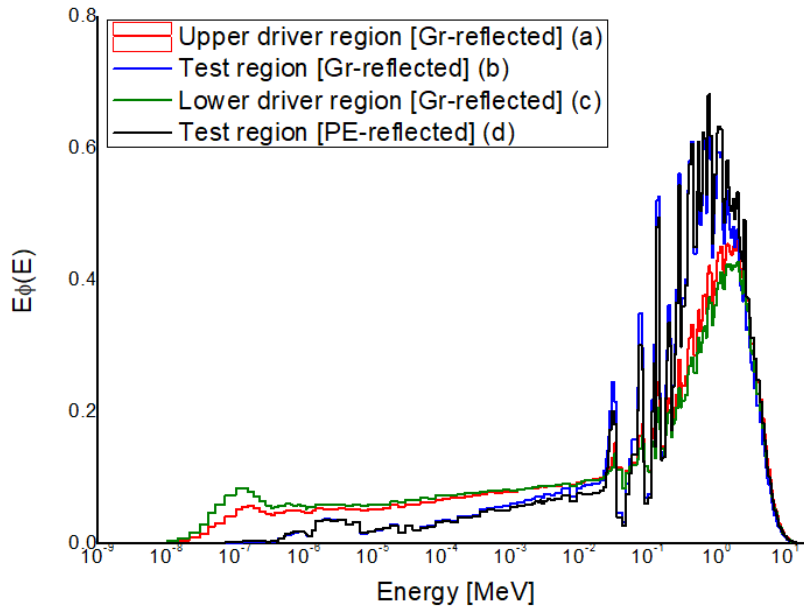


Fig. 3-15 Neutron spectra for (a) upper driver region [D60; Gr], (b) test region [T24; Gr], (c) lower driver region [D20; Gr] and (d) test region [T24; PE]

### 3.3.3 Neutronics Parameters

McCARD calculations are conducted to verify whether the Gr-reflected core can meet the safety regulations for implementation at the KUCA. To estimate the excess reactivity ( $\rho_{ex}$ ), control rod worth and secondary shutdown reactivity ( $\rho_{SD2}$ ), McCARD eigenvalue calculations are performed on 500 inactive and 1,000 active cycles with 100,000 histories per cycle using ENDF/B-VIII.0 cross section libraries. To assess the differential reactivity and ITC, McCARD eigenvalue calculations are performed on 500 inactive and 1,000 active cycles with 1,000,000 histories per cycle. When the ambient temperature is changed from 300 K to 350 K, the inserted reactivity is calculated by a direct subtraction.

The third column in Table 3-3 shows the McCARD calculation results. The excess reactivity is about 135 pcm. The secondary shutdown reactivity is about

14,000 pcm due to the big importance of the center region. It is noteworthy that ITC of the Gr-reflected core is 5.5 times smaller than that of PE-reflected core. From the table, one can see that the Gr-reflected hybrid spectrum core satisfies all the regulatory requirements.

Table 3-3 Regulatory requirements of KUCA A-core and McCARD calculation results of the Gr-reflected hybrid spectrum core

Contents	Regulations for KUCA A-core	McCARD results
$\rho_{ex}$	Less than 350 pcm	134.8±9.0 pcm
Control rod worth	$\rho_{ex} + 1000 \text{ pcm}$ $\leq \sum_i^3 (C_i \text{ rod worth})$	C1 rod worth: 2,124±13 pcm C2 rod worth: 1,773±13 pcm C3 rod worth: 1,509±13 pcm $\sum_i^3 (C_i \text{ rod worth})$ =5,406±22 pcm
	$(\text{Rod worth})_{\max}$ $\leq \frac{1}{3}(\text{All rod worth})$	$\frac{1}{3}(\text{All rod worth})$ =3,604±11 pcm
Differential reactivity	Differential reactivity at critical position $\leq 20 \text{ pcm/s}$ (Differential rod worth [pcm/cm] $\times$ inserted velocity [cm/s])	11.7±1.0 pcm/s (C1 rod)
$\rho_{SD2}$	More than 125% of $\rho_{ex}$	14,140±15 pcm
ITC	ITC $\leq 20 \text{ pcm/K}$	3.58±0.25 pcm/K

Figure 3-16 shows the integral rod worth curves for the Gr-reflected hybrid spectrum core. To estimate the differential rod worth at critical position, McCARD eigenvalue calculations are performed 500 inactive and 1,000 active cycles with 1,000,000 histories per cycle using ENDF/B-VIII.0 cross section libraries.

The critical position of the C1 rod, which has the largest rod worth, is 90 cm from the bottom. When the C1 rod is axially withdrawn from 85 cm to 90 cm, the inserted reactivity is conservatively calculated by a direct subtraction. The differential C1 rod worth at critical position is 14.6±1.0 pcm/cm. Differential

reactivity is calculated by multiplying the differential rod worth and its withdrawing velocity as much as 0.8 cm/s. The estimated differential reactivity of the C1 rod is  $11.7 \pm 1.0$  pcm/s.

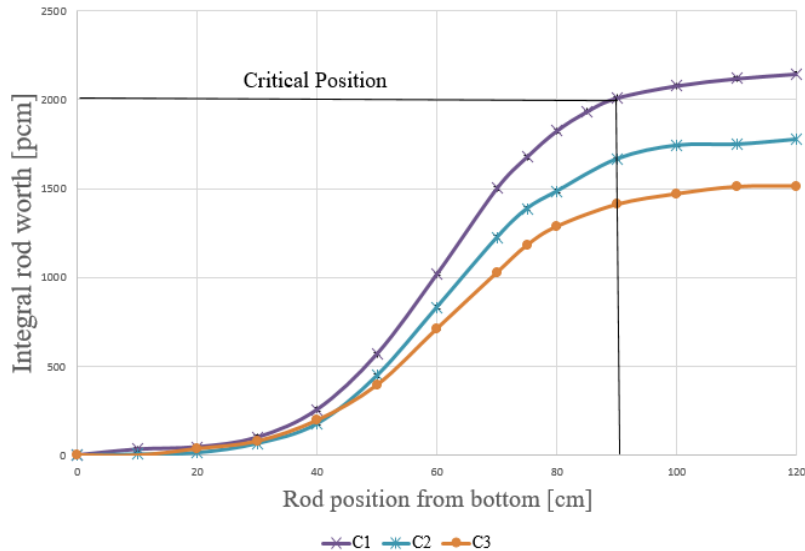


Fig. 3-16 Integral rod worth curve for the Gr-reflected hybrid spectrum core

The estimated ITC of the Gr-reflected core is  $3.58 \pm 0.25$  pcm/K and it is 5.5 times smaller than that of PE-reflected core. To analyze ITC, McCARD calculations for isotopic changes in microscopic cross sections are conducted. It is assumed that the effects of density changes due to thermal expansion are negligible because all regions consist of solid plates. McCARD eigenvalue calculations are performed on 500 inactive and 1,000 active cycles with 1,000,000 histories per cycle using ENDF/B-VIII.0 cross section libraries. The contribution of each isotope to ITC is calculated by a direct subtraction between 300 K and 350 K. For the contribution of the thermal scattering cross section of graphite ( $C_{TSL}$ ), the inserted reactivity is calculated by a direct subtraction between 296 K and 400 K.

Table 3-4 shows the contribution of the cross section changes of constituent isotopes in the divided regions to the ITC. Note that the ITC of each case can be obtained by summing up all the region-wise and isotope-wise contribution to ITC. From the table, one can see that the Doppler-broadening effect of uranium is negligible in the ITC. It is noteworthy that the contribution of the thermal scattering

cross section change of hydrogen in the reflector region is 3.8 times smaller than that of the PE-reflected core. Compared with the contribution of  $^1\text{H}_{\text{TSL}}$  in the reflector region, that of  $\text{C}_{\text{TSL}}$  to ITC is minor due to the small absorption cross section of carbon.

As shown in Table 3-4, the positive contribution of the thermal scattering cross section of hydrogen in the reflector region is dominant. It is caused by the spectrum hardening of the thermal neutrons. The spectral shift is attributable to a decrease in the absorption reaction of hydrogen in the reflector region while that of the moderator region decreases the fission reaction in the fuel region. The reduction of the absorption reaction increases the effective multiplication factor while that of the fission reaction decreases the effective multiplication factor.

Table 3-4 Region-wise and isotope-wise of each isotope to ITC of the Gr-reflected hybrid spectrum core

Region	Isotope	Contribution of each isotope to ITC [pcm/K] (RSD [%])
Fuel	$^{234}\text{U}$	-0.100 (190.0)
	$^{235}\text{U}$	-0.379 (50.0)
	$^{236}\text{U}$	-0.080 (237.2)
	$^{238}\text{U}$	-0.579 (33.0)
	$^{27}\text{Al}$	-0.379 (50.0)
Moderator	$^1\text{H}$	-0.100 (190.0)
	$^1\text{H}_{\text{TSL}}$	-1.657 (11.4)
	$^{12}\text{C}$	-0.040 (474.3)
	$^{13}\text{C}$	-0.160 (118.6)
Reflector	$^1\text{H}$	-0.080 (237.2)
	$^1\text{H}_{\text{TSL}}$	5.609 (3.4)
	$^{12}\text{C}$	0.020 (949.0)
	$^{13}\text{C}$	-0.080 (237.2)
	$\text{C}_{\text{TSL}}$	0.833 (10.9)
Total		2.830 (24.3)

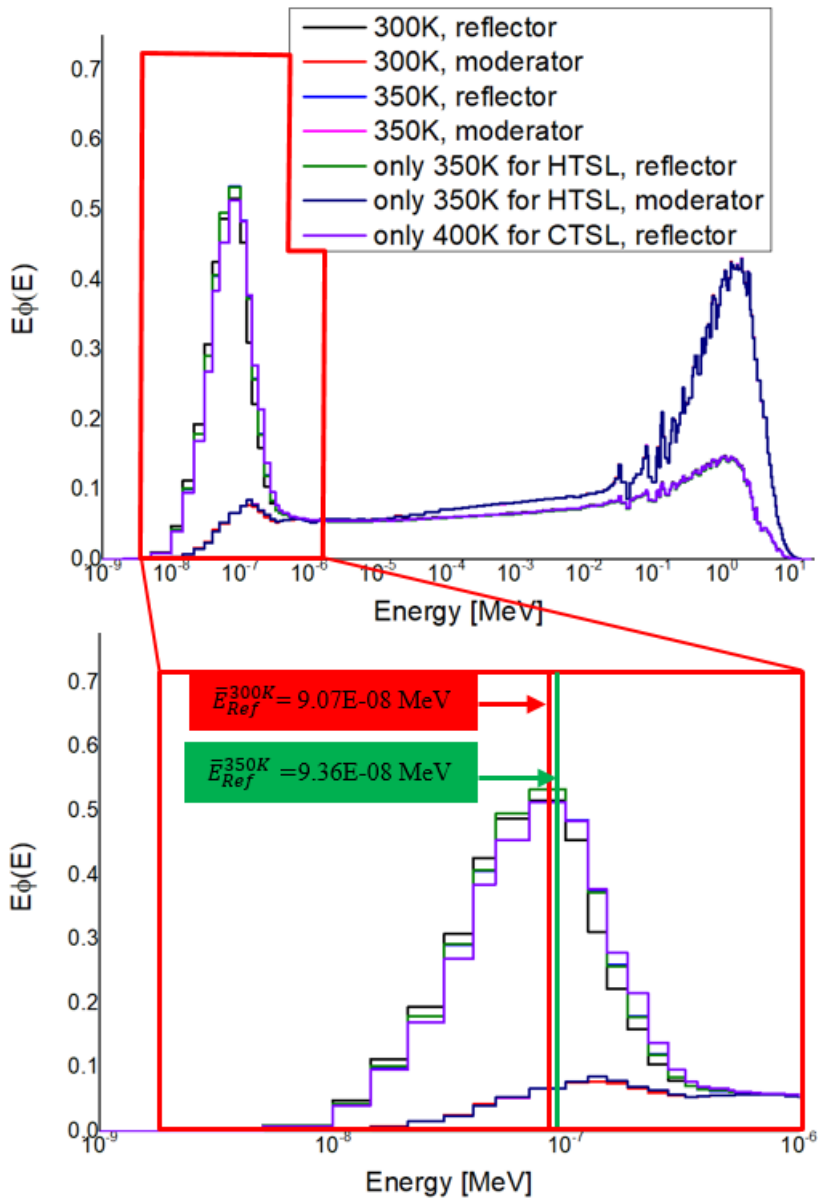


Fig. 3-17 Neutron spectra for the reflector and moderator regions of the Gr-reflected hybrid spectrum core at 300 K and 350 K

Figure 3-17 shows the neutron spectra for the reflector and moderator regions when the ambient temperature is 300 K and 350 K. From the figure, one can see that the neutron spectra in the thermal neutron range (less than 1.0 eV) are hardened as the ambient temperature is changed from 300 K to 350 K. Without considering the change of  $C_{TSL}$ , the average energy of thermal neutrons in the reflector region is changed from  $9.07E-08$  MeV to  $9.36E-08$  MeV. And, that of thermal neutrons in the

reflector region due to the change of  $^1\text{H}_{\text{TSL}}$  is  $9.35\text{E-}08$  MeV. The average thermal neutron energy in the reflector region of the Gr-reflected core is less hardened by 65 % than that of the PE-reflected one. The average energy of thermal neutrons in the reflector region of thermal neutrons due to the change of  $C_{\text{TSL}}$  from 296 K to 400 K is  $9.83\text{E-}08$  MeV. The average energy of thermal neutrons in the moderator region at 300 K and 350 K is changed from  $2.25\text{E-}07$  MeV to  $2.27\text{E-}07$  MeV. And, that of thermal neutrons due to the change of  $^1\text{H}_{\text{TSL}}$  in the moderator region is  $2.26\text{E-}07$  MeV.

The absorption cross sections of hydrogen and carbon are proportional to  $1/v$ . The thermal spectrum hardening in the moderator region decreases not only the absorption reaction of hydrogen in the moderator region but the fission reaction in the fuel region. The reduction of the absorption reaction increases the effective multiplication factor while that of the fission reaction decreases the effective multiplication factor. The contribution of the decrease in the fission reaction to ITC is more dominant than that in the absorption reaction to ITC because of the relatively small number of the PE plates used in the moderator region. Therefore, the contribution of the spectral shift effect in the moderator region to the ITC is negative.

The spectral shift is attributable to a decrease in the absorption reaction of carbon and hydrogen in the reflector region. The reduction of the absorption reaction increases the effective multiplication factor. Therefore, the contribution of the reflector element to the ITC is positive. By varying the reflector element from PE to Gr, the contribution of the spectral shift effect in the reflector to the ITC is reduced 3.4 times despite the positive contribution of  $C_{\text{TSL}}$  to the ITC.

From Fig. 2-17, one can see that the capture cross section of hydrogen is 100 times larger than that of carbon in the thermal neutron range. The inserted positive reactivity due to a decrease in the absorption reaction in the reflector region is reduced when the reflector element is changed from PE to Gr. Therefore, the contribution of the reflector element decreases from 21.3 pcm/K to 6.5 pcm/K due to the small absorption cross sections of  $^{12}\text{C}$  and  $^{13}\text{C}$ . With these results, one can see that Gr is an appropriate reflector element to reduce ITC.

# Chapter 4. Isothermal Temperature Coefficient

## 4.1 Sensitivity for ITC of System Temperature

To analyze sensitivity for ITC of the system temperature, the MC  $k$ -eigenvalue calculations are conducted for the hybrid spectrum core (Fig. 2-7) at six different system temperature points (303 K, 313 K, 323 K, 333 K, 343 K and 350 K). McCARD calculations are performed on 500 inactive and 1,000 active cycles with 1,000,000 histories per cycle using ENDF/B-VIII.0 cross section libraries. When the ambient temperature is changed from 300 K (Temp. 1) to the set temperature (Temp. 2), the inserted reactivity is calculated by a direct subtraction. In addition, the contribution of  $^1\text{H}_{\text{TSL}}$  to ITC is estimated at the six temperature points.

The effective multiplication factor increases linearly as the set temperature (Temp. 2) increases as shown in Fig. 4-1. From the figure, one can see that the contribution of the thermal scattering cross section change of hydrogen to  $k_{\text{eff}}$  is dominant due to the effect of the spectral shift of thermal neutrons.

Figure 4-2 shows the temperature-dependent ITC. The estimated ITCs between 300 K (Temp. 1) and the set temperatures (Temp. 2) exceed 20 pcm/K which is a regulatory requirement of KUCA A-core due to the dominant contribution of  $^1\text{H}_{\text{TSL}}$  to ITC.

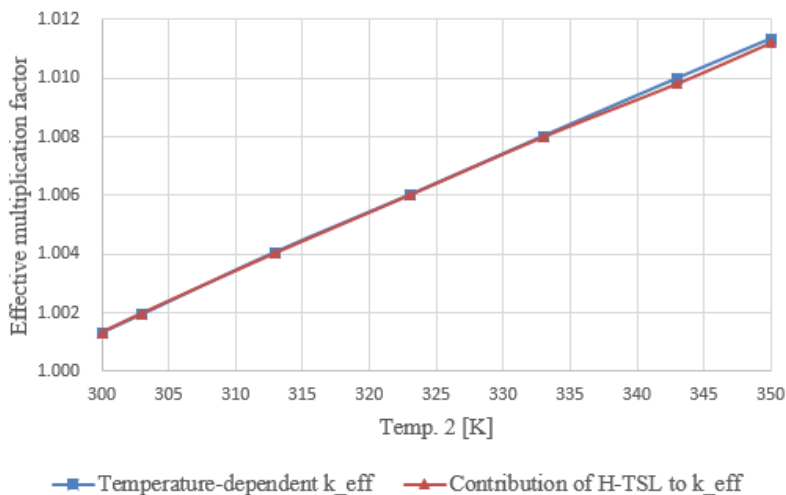


Fig. 4-1 Temperature-dependent  $k_{\text{eff}}$  for the hybrid spectrum core

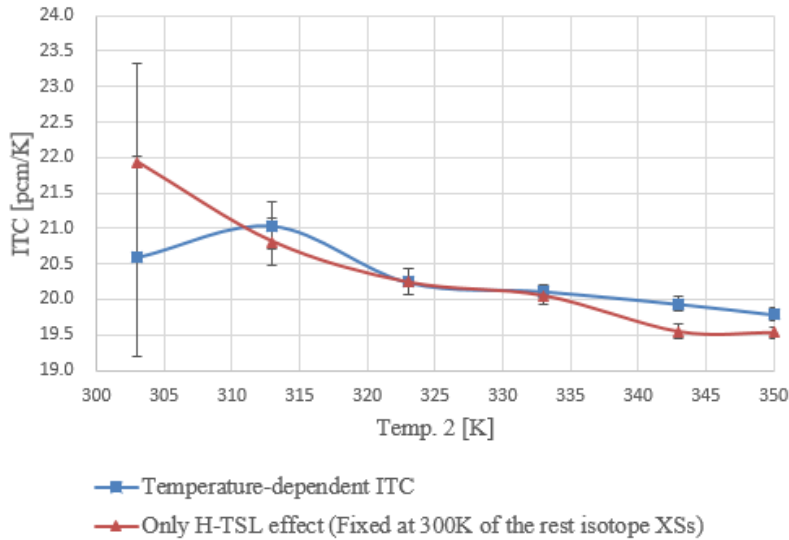


Fig. 4-2 Temperature-dependent ITC of the hybrid spectrum core

## 4.2 Sensitivity for ITC of Regional Reflector Element

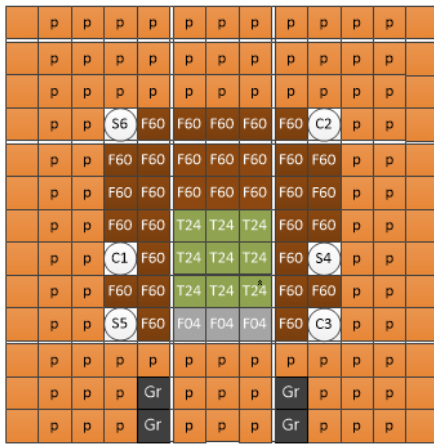
### 4.2.1 Hybrid Spectrum Core

In the previous chapter, the estimated ITCs of the hybrid spectrum core with the PE reflector according to the system temperature exceed the regulatory requirement of ITC. To reduce ITC, the reflector element used in the fuel assembly is suggested to change from PE to Gr as shown in Figs. 3-12 and 3-13. To assess the effect of the regional Gr-reflector, four cores are analyzed as shown in Fig. 4-3. Starting from the reference core (the hybrid spectrum core; Fig. 2-7), the Gr reflector rods are added as follows:

- (a) the reference core with the Gr-reflected fuel assemblies (D60, T24 and D04),
- (b) the core of (a) case radially surrounded by 1 layer of the Gr reflector rods,
- (c) the core of (a) case radially surrounded by 2 layers of the Gr reflector rods, and
- (d) the core of (a) case radially surrounded by 3 layers of the Gr reflector rods.

McCARD eigenvalue calculations are performed on 500 inactive and 1,000 active cycles with 100,000 histories per cycle using ENDF/B-VIII.0 cross section libraries. When the ambient temperature is changed from 300 K to 350 K, the inserted reactivity is calculated by a direct subtraction. The contribution of  $^1\text{H}_{\text{TSL}}$  to ITC is calculated by a direct subtraction between 300 K and 350 K. For the

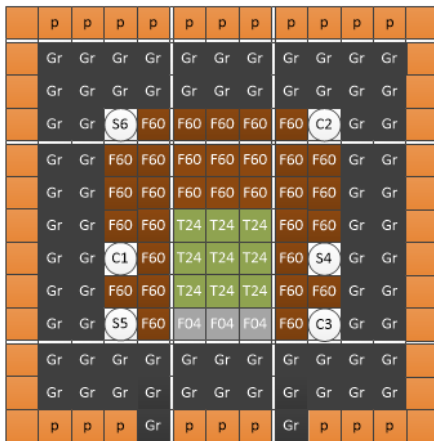
contribution of the thermal scattering cross section of graphite ( $C_{TSL}$ ), the inserted reactivity is calculated by a direct subtraction between 296 K and 400 K.



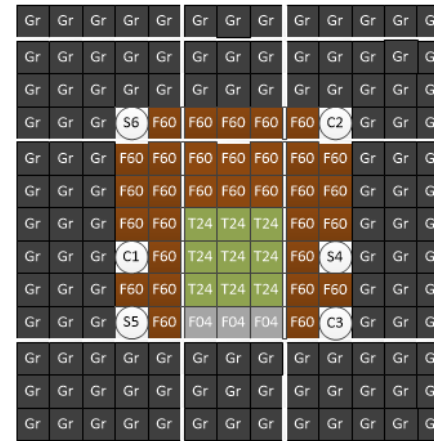
(a) Axial Gr-reflector in fuel assemblies



(b) Radial 1 layer of Gr reflector rods



(c) Radial 2 layers of Gr reflector rods



(d) Radial 3 layers of Gr reflector rods

Fig. 4-3 Core configurations of the hybrid spectrum core with the Gr reflectors

Tables 4-1 and 4-2 show the effective multiplication factor and ITC of the four cores, respectively. From Table 4-1, one can see that the effective multiplication factor increases as the surrounding Gr reflector rods increase because of the large moderating ratio of Gr. From Table 4-2, one can see that the estimated ITC decreases as the surrounding the PE reflectors decrease because of the large absorption cross section of hydrogen. And, the contribution of  $C_{TSL}$  to ITC is negligible, but that of  $C_{TSL}$  to ITC increases to 36% of the ITC when three layers of the Gr reflector rods radially surround the core (case (d)). From Table 4-2, the reflector element

surrounding the core can be suggested to change from PE to Gr to reduce ITC.

Table 4-1 Effective multiplication factor of the Gr-reflected hybrid spectrum cores

Case	Effective multiplication factor at 300 K
Reference	1.00131±0.00003
(a) axial	1.02401±0.00009
(b) 1 layer	1.07788±0.00009
(c) 2 layers	1.11561±0.00009
(d) 3 layers	1.14108±0.00009

Table 4-2 ITC of the Gr-reflected hybrid spectrum cores

Case	ITC [pcm/K]	Contribution of $^1\text{H}_{\text{TSL}}$ to ITC [pcm/K] (RSD [%])	Contribution of $\text{C}_{\text{TSL}}$ to ITC [pcm/K] (RSD [%])
Reference	19.80±0.09	19.54 (0.4)	0.01 (424.2)
(a) axial	13.38±0.27	13.54 (1.8)	-0.14 (84.9)
(b) 1 layer	7.07±0.24	7.08 (3.1)	-0.06 (181.8)
(c) 2 layers	3.67±0.23	3.75 (5.4)	0.37 (27.7)
(d) 3 layers	2.28±0.22	2.12 (9.2)	0.82 (11.9)

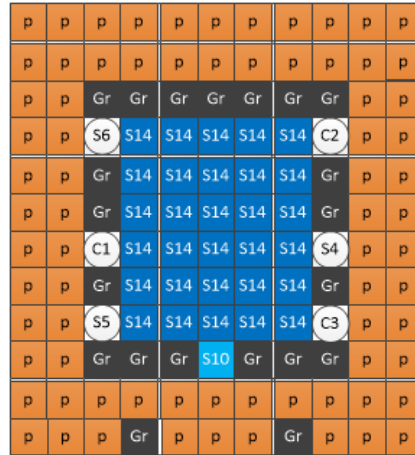
#### 4.2.2 Thermal Spectrum Core

The estimated ITC of the PE-reflected thermal spectrum core (Fig. 2-4) is closed to the regulatory requirement of ITC. To reduce ITC, the reflector element used in the fuel assembly is suggested to change from PE to Gr as shown in Fig. 2-11. To assess the effect for the regional Gr-reflector, four cores are analyzed as shown in Fig. 4-4. Starting from the reference core (thermal spectrum core; Fig. 2-4), the Gr reflector rods are added as follows:

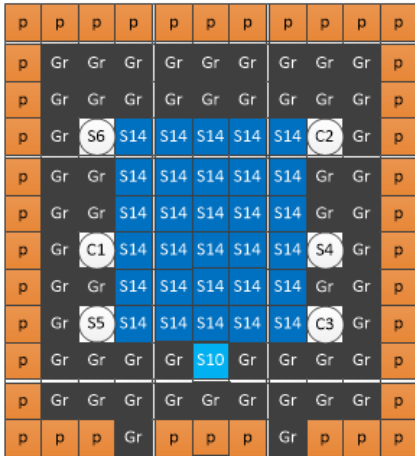
- (a) the reference core with the Gr-reflected fuel assemblies (S14 and S10),
- (b) the core of (a) case radially surrounded by 1 layer of the Gr reflector rods,
- (c) the core of (a) case radially surrounded by 2 layers of the Gr reflector rods, and
- (d) the core of (a) case radially surrounded by 3 layers of the Gr reflector rods.



(a) Axial Gr-reflector in fuel assemblies



(b) Radial 1 layer of Gr reflector rods



(c) Radial 2 layers of Gr reflector rods



(d) Radial 3 layers of Gr reflector rods

Fig. 4-4 Core configurations of thermal spectrum core with the Gr reflectors

McCARD eigenvalue calculations are performed on 500 inactive and 1,000 active cycles with 100,000 histories per cycle using ENDF/B-VIII.0 cross section libraries. When the ambient temperature is changed from 300 K to 350 K, the inserted reactivity is calculated by a direct subtraction. The contribution of  $^1H_{TSL}$  to ITC is calculated by a direct subtraction between 300 K and 350 K. For the contribution of the thermal scattering cross section of graphite ( $C_{TSL}$ ), the inserted reactivity is calculated by a direct subtraction between 296 K and 400 K.

Tables 4-3 and 4-4 show the  $k_{eff}$  and ITC of the four cores, respectively. From Table 4-3, one can see that  $k_{eff}$  increases as the surrounding the Gr reflector rods increase because of the large moderating ratio of Gr. It is noteworthy that the

estimated ITC of the thermal spectrum core gradually decreases as the surrounding PE reflectors decrease, compared with that of the hybrid spectrum core. The positive contribution of the moderator element to ITC of the thermal spectrum core is larger than that of the hybrid spectrum core because relatively many PE plates are used in the moderator region in the thermal spectrum core. The contribution of  $C_{TSL}$  to ITC is still negligible. With these results, it can be concluded that the reflector element surrounding the core can be suggested to change from PE to Gr reflector to reduce ITC.

Table 4-3 Effective multiplication factor of the Gr-reflected thermal spectrum cores

Case	Effective multiplication factor at 300 K
Reference	$1.00082 \pm 0.00002$
(a) axial	$1.00718 \pm 0.00008$
(b) 1 layer	$1.03540 \pm 0.00008$
(c) 2 layers	$1.06171 \pm 0.00008$
(d) 3 layers	$1.07789 \pm 0.00008$

Table 4-4 ITC of Gr-reflected thermal spectrum cores

Case	ITC [pcm/K]	Contribution of ${}^1H_{TSL}$ to ITC [pcm/K] (RSD [%])	Contribution of $C_{TSL}$ to ITC [pcm/K] (RSD [%])
Reference	$19.61 \pm 0.10$	19.47 (1.2)	-0.02 (412.3)
(a) axial	$18.90 \pm 0.25$	18.88 (1.7)	0.02 (565.7)
(b) 1 layer	$16.18 \pm 0.22$	16.35 (1.2)	0.05 (226.3)
(c) 2 layers	$13.84 \pm 0.22$	13.74 (1.5)	0.33 (28.7)
(d) 3 layers	$13.10 \pm 0.22$	12.31 (1.6)	0.88 (11.1)

## Chapter 5. Conclusion

In this research, the solid-moderated cores using the LEU modeling fuel assembly are designed as a feasibility study for the LEU conversion at KUCA A-core. The LEU modeling unit cell stacked in the LEU modeling fuel assembly is composed of four HEU plates and one NU plate to have an enrichment of 17.0 wt% as the unit cell average value. The two solid-moderated cores with the thermal spectrum and the fast-thermal hybrid spectrum are designed with the LEU modeling fuel assembly. The cores are designed to use less than 5,000 HEU plates and meet the safety regulations for implementation at the KUCA. In this research, the cores with the LEU modeling fuel is designed by McCARD. McCARD calculations are conducted to estimate the excess reactivity ( $\rho_{ex}$ ), control rod worth and secondary shutdown reactivity ( $\rho_{SD2}$ ), the differential reactivity and the isothermal temperature coefficient (ITC).

The thermal spectrum core is designed with the LEU modeling fuel. The ratio of  $^1\text{H}$  to  $^{235}\text{U}$  in the LEU modeling unit cell is set to 200 or higher to make a thermal spectrum. The LEU modeling unit cell used in the fuel assembly (S14) is composed of four HEU plates, one NU plate and nine PE plates. The thermal spectrum core is composed of 30 S14 assemblies and one S10 assembly. The total number of HEU plates used in the core is 1,720 plates. A softened spectrum is achieved in the thermal spectrum core. And, the thermal spectrum core satisfies all the regulatory requirements but the large ITC as much as  $19.63 \pm 0.06$  pcm/K is closed to the regulatory requirement of ITC. The large ITC is caused by the effect of the spectral shift of thermal neutrons. To reduce ITC, the reflector element is changed from polyethylene (PE) to graphite (Gr). By varying the reflector element from PE to Gr, the ITC decreases to 13.5 pcm/K. Also, the thermal spectrum core with the Gr reflector satisfies all the regulatory requirements. From the design analyses, the thermal spectrum core is found feasible with the use of the LEU modeling fuel at KUCA.

The LEU modeling fuel assembly used in the fast-thermal hybrid spectrum core is designed without the PE plates to make a fast spectrum. The designed hybrid spectrum core has two different regions because the core with the only LEU

modeling fuel assemblies is hard to reach criticality. The test region is composed of 9 T24 assemblies which are composed of 24 LEU modeling unit cells and the driver region consists of 31 D60 and 3 D04 assemblies to have the core reach its critical mass. The total number of HEU plates used in the core is 4,608 plates. Compared to the spectrum of the thermal spectrum core, a hardened spectrum is achieved in the test region of the hybrid spectrum core. The hybrid spectrum core satisfies all the regulatory requirements except ITC considering its 95% confidence intervals. The large ITC as much as  $19.79 \pm 0.08$  pcm/K is caused by the effect of the spectral shift of thermal neutrons. To reduce ITC, the Gr-reflected hybrid spectrum core is designed. By varying the reflector element from PE to Gr, the ITC decreases to 3.6 pcm/K. From the design analyses, the LEU modeling fuel assembly without the moderator present difficulty in achieving criticality in the fast spectrum core but the fast-thermal hybrid spectrum core is found feasible with the use of the LEU modeling fuel at KUCA.

To analyze sensitivity for ITC of the system temperature, McCARD calculations are conducted for the hybrid spectrum at six different system temperatures. The estimated ITCs exceed 20 pcm/K which is the regulatory requirement of ITC. To assess the effect of the regional Gr reflector, four cores are analyzed. The estimated ITC decreases as the surrounding PE reflectors decrease. With the above results, it can be concluded that the reflector element surrounding the core can be suggested to change from PE to Gr reflector to reduce ITC.

# References

1. Travelli, A., “Current Status of the RERTR Program,” ANL/RERTR/TM—3, International Atomic Energy Agency (1983).
2. Durand, J.P. and Fanjas, Y., “LEU fuel development at CERCA: status as of October 1993,” Proc. 16th Int. Meet. on Reduced Enrichment for Research and Test Reactors. Japan Atomic Energy Research Institute Report, Oarai, Japan, JAERI-M 94-02, pp. 71–78 (1994).
3. J. L. SNELGROVE et al., “Development of Very-High-Density Low-Enriched-Uranium Fuels,” Nucl. Eng. Des., 178, 119 (1997).
4. G. Ball, O. Knoesen and A. Kocher, “Status Update on Conversion to LEU Based <sup>99</sup>Mo Production in South Africa,” RERTR 2011, Santiago, Chile, Oct 23-27 (2011).
5. H. C. Odoi et al., “Conversion of International MNSR – Reference Case of Ghana MNSR,” RERTR 2012, Warsaw, Poland (2012).
6. Unesaki H et al., “Neutronic Analysis for Utilization of Low Enriched Uranium Fuel at Light Water Moderated/Reflected Core of Kyoto University Critical Assembly (KUCA),” RERTR 2012, Warsaw, Poland (2012).
7. S. H. KIM et al., “A Feasibility Study on Fast Reactor with Low-Enriched Uranium Fuel at Kyoto University Critical Assembly,” Prog. Nucl. Energy, 100, 60 (2017).
8. H. J. SHIM et al., “McCARD: Monte Carlo Code for Advanced Reactor Design and Analysis,” Nucl. Eng. Technol., 44, 161 (2012).
9. D. A. Brown et al., “ENDF/B-VIII.0: the 8<sup>th</sup> Major Release of the Nuclear Reaction Data Library with CIELO-project Cross Sections, New Standards and Thermal Scattering Data,” Nuclear Data Sheets, 148, 1 (2018).
10. C. H. PYEON et al., “Uncertainty Quantification of Criticality in Solid-Moderated and –Reflected Cores at Kyoto University Critical Assembly,” J. Nucl. Sci. Technol., 55, 812 (2018).
11. R. MacFARLANE and D. W. MUIR, et al., “The NJOY Nuclear Data Processing System, Version 2016,” Tech. Rep. LA-UR-17-20093, Los Alamos National Laboratory, (2017).
12. S. SHIROYA, M. MORI, and K. KANDA, “Analysis of Experiment on Temperature Coefficient of Reactivity in LightWater-Moderated and Heavy-Water-Reflected Cylindrical Core Loaded with Highly-Enriched-Uranium or Medium-EnrichedUranium Fuel,” J. Nucl. Sci. Technol., 33, 3, 211 (1996);

<http://dx.doi.org/10.1080/18811248.1996.9731892>.

13. B. K. Jeon, C. H. PYEON, and H. J. SHIM, "Monte Carlo Perturbation Analysis of Isothermal Temperature Reactivity Coefficient in Kyoto University Critical Assembly," *Nuclear Technology*, 191:2, 174-184 (2017), DOI: 10.13182/NT14-83.
14. C. H. Pyeon, "Experimental Benchmarks of Neutronics on Solid Pb-Bi in Accelerator-Driven System with 100 MeV Protons at Kyoto University Critical Assembly," KURRI-TR-447, Research Reactor Institute, Kyoto University (2017).

## Appendix

### A. Atomic Number Density

Table A-1. Atomic densities of polyethylene (PE) plates [14]

Material	Isotope	Atomic Density [ $\times 10^{24}/\text{cm}^3$ ]
1/2" thick plate (12.500 mm)	$^1\text{H}$	8.06560E-02
	C	4.03280E-02
1/4" thick plate (6.300 mm)	$^1\text{H}$	8.08711E-02
	C	4.04356E-02
1/8" thick plate (3.086 mm)	$^1\text{H}$	8.02167E-02
	C	4.01084E-02

Table A-2. Atomic densities of polyethylene (p) plates [14]

Material	Isotope	Atomic Density [ $\times 10^{24}/\text{cm}^3$ ]
1/8" thick plate (p)	$^1\text{H}$	7.77938E-02
	C	3.95860E-02
10" long rod (p)	$^1\text{H}$	7.97990E-02
	C	4.08960E-02

Table A-3. Atomic densities of graphite (Gr)

Material	Isotope	Atomic Density [ $\times 10^{24}/\text{cm}^3$ ]
Graphite (Gr)	$^{12}\text{C}$	8.51111E-02
	$^{13}\text{C}$	9.55337E-04

## B. Partial Fuel Assemblies and Reflector Rods

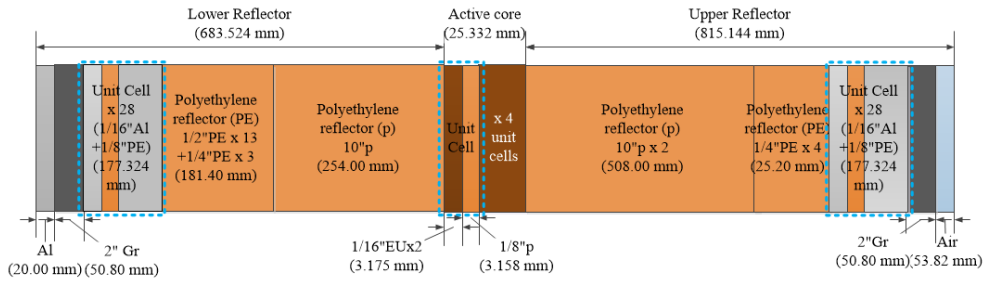


Fig. B-1 The D04 assembly used in hybrid spectrum core

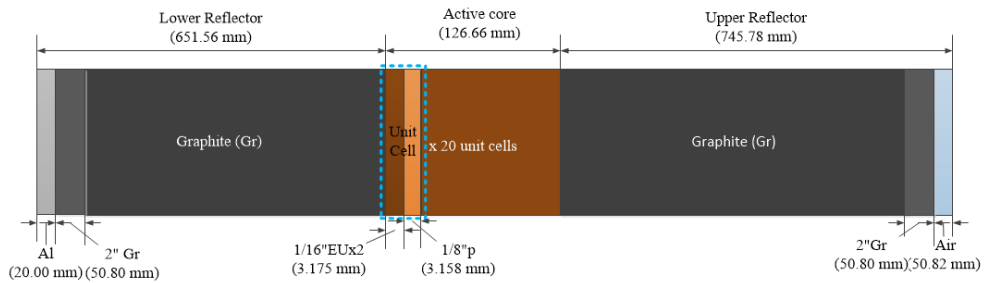


Fig. B-2 The D20 assembly used in Gr-reflected hybrid spectrum core

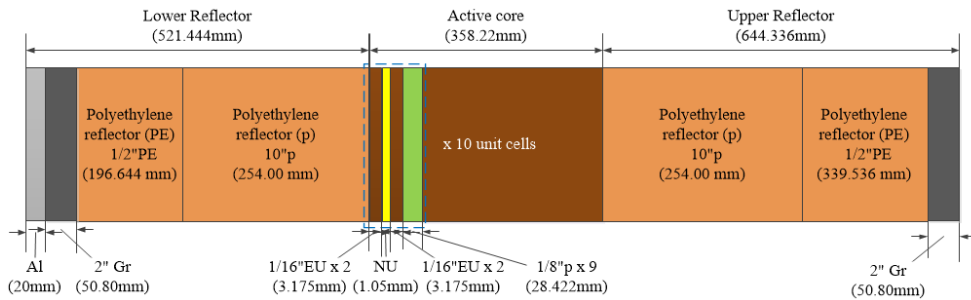


Fig. B-3 the S10 assembly used in thermal spectrum core

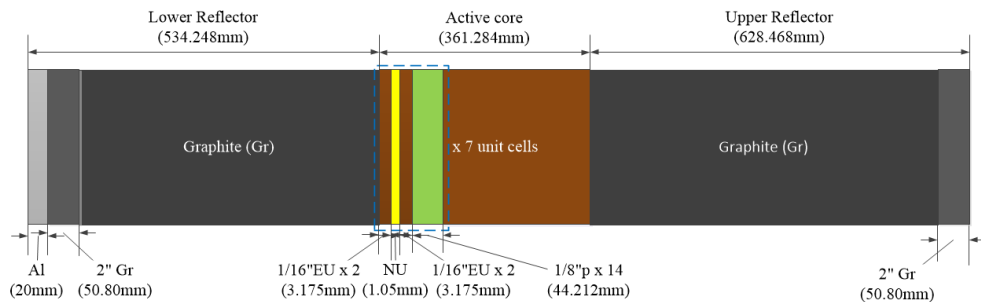


Fig. B-4 The S07 assembly used in Gr-reflected thermal spectrum core

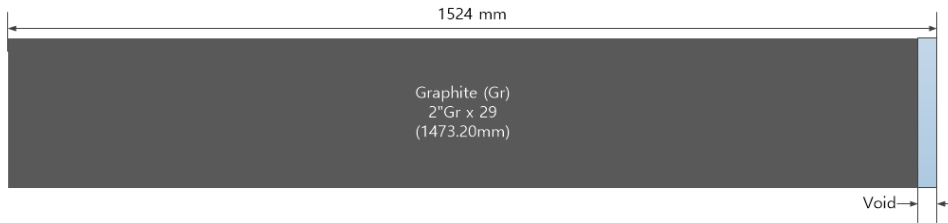


Fig. B-5 The Gr reflector rod

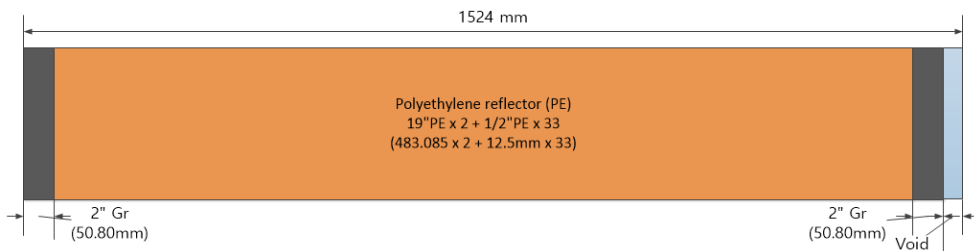


Fig. B-6 The outer PE reflector rod

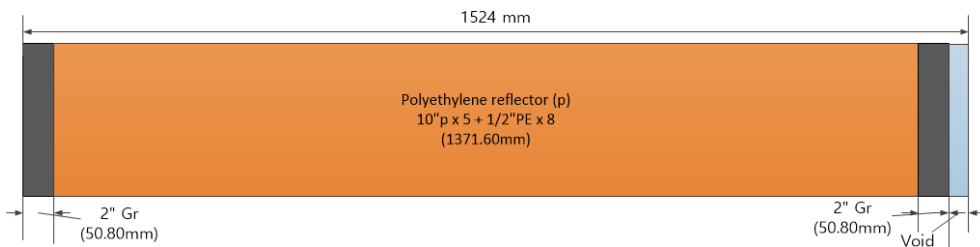


Fig. B-7 The inner PE reflector rod

## 초 록

최근 교토대 임계집합체에서는 고농축우라늄 핵연료 대신 저농축우라늄 핵연료를 이용한 전환 노심 연구가 진행되고 있다. 본 연구는 교토대 임계집합체 고체 감속 노심에 대하여 저농축우라늄 핵연료 전환 노심의 실현가능성을 알아보기 위해 고농축 및 천연 우라늄 판으로 이루어진 저농축 모의 핵연료를 이용하여 열중성자 에너지스펙트럼 노심과 고속-열중성자 에너지스펙트럼 혼합 노심을 설계하였다. 노심 설계에 사용되는 고농축 우라늄 판의 수를 5,000장 미만으로 설정하였다. 본 연구에서는 몬테칼로 입자수송해석 코드인 McCARD를 이용하여 노심을 설계하였다. 노심의 임계도 및 중성자 에너지스펙트럼을 해석하기 위해 McCARD 계산이 수행되었으며, 설계 노심의 교토대 임계집합체 설계 제한조건 만족 여부를 파악하였다.

저농축 모의 핵연료를 이용한 열중성자 에너지스펙트럼 노심을 설계하였다. 열중성자 에너지스펙트럼을 갖도록 저농축 모의 핵연료 기본단위 셀의 수소와 우라늄-235 비를 200 이상으로 설정하였다. 해당 저농축 모의 핵연료 기본단위 셀은 4장의 고농축우라늄, 1장의 천연우라늄 그리고 9장의 폴리에틸렌 판으로 이루어져 있다. 열중성자 에너지스펙트럼 노심은 31개의 저농축 모의 핵연료로 이루어져 있다. 해당 노심에 사용된 고농축핵연료 판은 총 1,720장이다. 교토대 임계집합체의 대표 고체 감속 노심인 EE1과 비교하였을 때, 해당 노심이 더 연화된 중성자 에너지스펙트럼을 보였다. 해당 노심의 잉여반응도, 제어봉가, 추가 정지반응도, 미분 반응도(제어봉이 임계 지점을 지날 때 초당 삽입되는 미분제어봉가) 및 등온온도계수를 구하기 위해 McCARD 계산을 수행하였다. 열중성자 에너지스펙트럼 노심은 설계 제한조건들을 모두 만족하였으나 등온온도계수는 설계제한조건치 20 pcm/K에 근접하였다. 등온온도계수를 줄이기 위해 반사체 물질로 폴리에틸렌 대신 흑연 사용을 제안하였다. 반사체 물질로 폴리에틸렌 대신 흑연을 사용할 때, 등온온도계수는 19.6 pcm/K에서 13.5 pcm/K로 감소하였다. 또한 흑연 반사체를 사용한 열중성자 에너지스펙트럼 노심은 모든 설계 제한조건을 만족하였다. 본 연구는 저농축 모의 핵연료를 이용한 교토대 임계집합체 열중성자 에너지스펙트럼 노심의 실현가능성을 확인하였다.

고속-열중성자 에너지스펙트럼 혼합 노심에 사용된 저농축 모의 핵연료

집합체는 고속중성자 에너지스펙트럼을 갖도록 감속재가 없이 설계되었다. 저농축 모의 핵연료 집합체만으로 이루어진 노심은 임계에 도달하기 어렵다. 따라서, 고속-열중성자 에너지스펙트럼 혼합 노심은 두 영역으로 나뉜다. 하나는 저농축 모의 핵연료가 사용되는 시험 영역이다. 다른 하나는 노심이 임계에 도달할 수 있도록, 교토대 임계집합체의 대표 노심에 사용되는 고농축핵연료집합체로 이루어진 운전 영역이다. 해당 노심에 사용되는 고농축우라늄 판의 수는 총 4,608장이다. 열중성자 에너지스펙트럼 노심과 비교하였을 때, 설계 노심의 시험 영역이 더 경화된 중성자 에너지스펙트럼을 보였다. 해당 노심은 모든 설계 제한조건을 만족하였으나 등온온도계수의 경우 95% 신뢰구간에서 설계제한조건을 만족하였다. 등온온도계수를 줄이기 위해 노심에 사용되는 반사체 물질을 폴리에틸렌에서 흑연으로 교체하였다. 반사체 물질로 폴리에틸렌 대신 흑연을 사용할 때, 등온온도계수는 19.8 pcm/K에서 3.6 pcm/K로 감소하였다. 또한, 흑연 반사체를 이용한 고속-열중성자 에너지스펙트럼 혼합 노심은 등온온도계수를 포함한 설계 제한조건들을 모두 만족하였다. 고속중성자 에너지스펙트럼 노심의 경우 감속재가 없는 저농축 모의 핵연료만으로 임계 도달하기 어려우나, 교토대 임계집합체 고속-열중성자 에너지스펙트럼 노심의 실현가능성을 확인하였다.

시스템 온도에 따른 등온온도계수 민감도를 분석하기 위해, 서로 다른 온도에 대하여 고속-열중성자 에너지스펙트럼 혼합 노심의 몬테칼로  $k$ -고유치 계산을 수행하였다. 열중성자의 평균에너지 증가 효과 때문에 추정된 등온온도계수가 설계 제한조건 20 pcm/K을 넘는 것을 확인하였다. 등온온도계수 감소를 위해 영역별로 폴리에틸렌에서 흑연 반사체로 바꾼 네 가지 노심을 선정하여 분석하였다. 노심 분석 결과를 통해, 등온온도계수를 낮추기 위한 방법으로 폴리에틸렌보다 흑연이 반사체 물질로 적합하다는 사실을 도출하였다.

**주요어:** 저농축우라늄 모의 핵연료, 천연 우라늄, 교체-감속 노심, 중성자에너지스펙트럼, 등온온도계수, 교토대 임계집합체, McCARD

**학번:** 2018-28054